Themed Issue: New discoveries and perspectives in mental and pain disorders

THEMED ISSUE ARTICLE

Long-term molecular differences between resilient and susceptible mice after a single traumatic exposure

Diego Pascual Cuadrado[1] 🔵 | Hristo Todorov[2] | Raissa Lerner[1] | Larglinda Islami[3] | Laura Bindila[1] | Susanne Gerber[2] | Beat Lutz[1,3]

[1]Institute of Physiological Chemistry, University Medical Center of the Johannes Gutenberg University, Mainz, Germany

[2]Institute of Human Genetics, University Medical Center of the Johannes Gutenberg University, Mainz, Germany

[3]Group Molecular and Cellular Mechanisms of Resilience, Leibniz Institute for Resilience Research, Mainz, Germany

Correspondence
Dr Beat Lutz, Institute of Physiological Chemistry, University Medical Center of the Johannes Gutenberg University, Mainz, Germany.
Email: beat.lutz@uni-mainz.de

Background and Purpose: Post-traumatic stress disorder (PTSD) is a heterogeneous disorder induced by trauma, resulting in severe long-term impairments of an individual's mental health. PTSD does not develop in every individual and, thus, some individuals are more resilient. However, the underlying molecular mechanisms are poorly understood. Here, we aimed to elucidate these processes.

Experimental Approach: We used a single-trauma PTSD model in mice to induce long-term maladaptive behaviours and profiled the mice 4 weeks after trauma into resilient or susceptible individuals. The classification of phenotype was based on individual responses in different behavioural experiments. We analysed microbiome, circulating endocannabinoids, and long-term changes in brain phospholipid and transcript levels.

Key Results: We found many molecular differences between resilient and susceptible individuals across multiple molecular domains, including lipidome, transcriptome and gut microbiome. Some differences were stable even several weeks after the trauma, indicating the long-term impact of traumatic stimuli on the organism's physiology. Furthermore, the integration of these multilayered molecular data revealed that resilient and susceptible individuals have very distinct molecular signatures across various physiological systems.

Conclusion and Implications: Trauma induced individual-specific behavioural responses that, in combination with a longitudinal characterisation of mice, could be used to identify distinct sub-phenotypes within the trauma-exposed group. These groups differed significantly not only in their behaviour but also in specific molecular aspects across a variety of tissues and brain regions. This approach may reveal new targets and predictive biomarkers for the pharmacological treatment and prognosis of stress-related disorders.

Abbreviations: 2-AG, 2-arachidonoyl glycerol; ASR, acoustic startle response; CA, cornus ammonis; CAP, constrained analysis of principal coordinates; CF, contextual fear; DAGLα, diacylglycerol lipase α; DG, dentate gyrus; ECS, endocannabinoid system; FAAH, fatty acid amide hydrolase; FS, foot-shock; GF, generalized fear; HbT, holeboard test; HPA, hypothalamic–pituitary–adrenal; NAPE-PLD, N-acylphosphatidylethanolamine-phospholipase D; PFC, prefrontal cortex; PTSD, post-traumatic stress disorder; SIT, social interaction test; sPLS-DA, sparse partial least squares discriminant analysis; SPT, sucrose preference test.

Diego Pascual Cuadrado and Hristo Todorov contributed equally to this study.

1 | INTRODUCTION

Post-traumatic stress disorder (**PTSD**) is a mental disorder that develops after an individual is exposed to a traumatic experience, such as warfare, deadly accidents or sexual violence. The symptoms associated with the disorder cause a severe and chronic impairment of the individual's daily life quality. They include, among others, intrusive memories, hypervigilance and avoidance of trauma-related cues (American Psychiatric Association, 2013). In contrast to other stress- and trauma-induced disorders, the symptoms of PTSD usually appear after an incubation period of approximately 1 month. They can last for years but only affect a relatively small percentage of the individuals exposed to trauma. Other mood disorders, such as **anxiety** or **depression**, show high co-morbidity with PTSD (Walter et al., 2018). Due to the heterogeneity of PTSD symptomatology, PTSD can be considered as a spectrum disorder with different pathological phenotypes (Guina et al., 2017).

Research on the molecular aspects underlying PTSD has uncovered a plethora of dysregulated systems across the organism. For instance, a hyperresponsive hypothalamic–pituitary–adrenal (HPA) axis has been shown to be the cause of increased levels of **corticotrophin-releasing hormone (CRH)**, linked with hypervigilant behaviour and reduced sensorimotor gating (Flandreau et al., 2015), as well as overconsolidation of fear memories (Thoeringer et al., 2012). PTSD also compromises the immune system, as shown by increased pro-inflammatory interleukins in PTSD patients, such as **IL-6**, **IL-1β** and **TNF-α**, and other markers of inflammation (Menard et al., 2017). Following the suggestion of a link between microbial communities in the gut and the HPA axis (Sudo et al., 2004), it was shown that the gut microbiome influences brain processes such as fear recall (Hoban et al., 2018) and extinction learning (Chu et al., 2019), suggesting that the gut microbiome may modulate the predisposition to and severity of PTSD. However, further research on the gut microbiome is required to understand how changes in the gut microbial community affect its host's behaviour and physiology (Kelly et al., 2015). Another important structural element of brain function is phospholipids. These lipids form the cell membrane, making them abundant, easily accessible and involved in cellular signalling processes. Phospholipids are, for example, also involved in the formation of lipid rafts, the functionality of membrane receptors and neurotransmission. Despite the known roles of phospholipids on brain homeostasis and apoptosis, among others, they tend to be overlooked in psychiatric research. Another system that uses lipids as signalling molecules, the endocannabinoid system (ECS), is also dysregulated in

What is already known

- Trauma-induced disorders are very heterogeneous pathologies that affect exposed individuals very differently.
- There is a problem of translatability between animal models of trauma and human pathologies.

What does this study add

- Our results suggest novel strategies to study trauma-exposed individuals based on their individual behavioural performance.
- They also provide molecular insights into the differences underlying resilience to trauma and PTSD-like pathology.

What is the clinical significance

- Increased understanding of the molecular mechanisms underlying resilience to trauma at different molecular levels.
- Longitudinal classification based on individual performance across different behavioural domains.

different brain regions of PTSD patients (Morena et al., 2018). The ECS is especially relevant in the prefrontal cortex (PFC), as neuronal activity in this region is negatively correlated with PTSD symptoms (Williams et al., 2006), and is involved in the inhibition of CRH release from the hypothalamic paraventricular nucleus in a **cannabinoid CB₁ receptor**-dependent manner (Herman et al., 2016). Given the role of the ECS in regulating homeostasis in various contexts, this modulatory system has become a research focus for its potential in preventing or treating stress-related disorders (Sbarski & Akirav, 2020).

As mentioned above, not all individuals that are exposed to trauma develop maladaptive behaviour related to PTSD. This feature is called resilience and is known as the dynamic ability of an individual to overcome adversity, trauma, or significant threat, in order to return, successfully, to the mental state prior to the stress

experience (Horn & Feder, 2018). Despite its relevance (Rakesh et al., 2019), very little is known about the underlying mechanisms of resilience (or susceptibility) to stressful experiences. The predisposition to PTSD appears to be influenced by a wide range of factors, including genetics (Nievergelt et al., 2019) and type of trauma (Cowden Hindash et al., 2019),. Research on the neurobiology of PTSD has been hindered due to the intrinsic heterogeneity of PTSD symptoms, but also due to limiting factors of current PTSD models, impeding their translatability. Some of these limitations, such as studying only one gender, analysing the average group response or classifying animals based on a single behavioural domain, can be overcome but require particular consideration in the experimental planning. However, other limitations, such as risk factors originating from epigenetic alterations induced by past experiences, the gut microbiome and the reactivity of the HPA axis, are poorly understood (Richter-Levin et al., 2019). In our study, we aimed at implementing a trauma model capable of inducing long-lasting maladaptive behaviour across several behavioural domains. We have combined this model with a longitudinal behavioural survey to profile those mice that showed a consistent behavioural response similar to (i.e., resilient phenotype) or different to (i.e., susceptible phenotype) unexposed individuals. We show here that this approach can provide new insights into the molecular differences and possible underlying mechanisms between the trauma-exposed individuals that overcome the trauma and those that fail.

2 | METHODS

2.1 | Mouse line

All animal care and experimental procedures were conducted in accordance with the European Community's Council Directive of 22 September 2010 (2010/63EU) and approved by the respective agency of Rhineland-Palatinate State, Germany (Landesuntersuchungsamt, Permit Number G17-1-027). Animal studies are reported in compliance with the ARRIVE guidelines (Percie du Sert et al., 2020) and with the recommendations made by the *British Journal of Pharmacology* (Lilley et al., 2020).

All experimental procedures were carried out with the heterozygous double transgenic mouse line Arc-CreER^{T2} × R26-CAG-LSL-Sun1-sfGFP-myc, which has been described previously (Mo et al., 2015). Male mice were 8 ± 1 weeks old at the time of trauma. Mice were singly housed 2 weeks before the start of the experiment and for the entire duration of the study. Food and water were provided ad libitum, and mice were subjected to a 12-h light–dark cycle (7:00 AM to 7:00 PM). For sample collection, mice were decapitated while under isoflurane anaesthesia. The number of animals in the control (−FS) and trauma-exposed (+FS) groups was balanced in a proportion of 1:5 (−FS:+FS) in order to acquire a minimum number of trauma-exposed animals with extreme behaviours (resilient and susceptible) for a meaningful molecular analysis. Mice were randomly assigned to either the −FS or +FS groups.

2.2 | Trauma model

To induce a strong and reliable PTSD-like phenotype, we used a modified version of the protocol developed by Siegmund and Wotjak (2007). In summary, the mouse was placed in the shock chamber of a fear conditioning set-up (Med Associates; square, 15 × 20 cm, grid floor) and left to habituate for 3 min with lights on. Afterwards, two inescapable scrambled foot-shocks (FS, 1.5 mA; 2 s) were delivered to the paws through the bottom grid, with 1 min of rest between each shock. After the second electric shock, the mouse was left for one more minute in the chamber and then returned to its home cage. The behaviour during the FS protocol was monitored using video cameras. The shock chamber was cleaned after every recording using 1% acetic acid. Trauma-exposed mice were designated as +FS mice. Non-shocked mice (−FS mice) were exposed in parallel to the same chamber and underwent the same protocol, but without a foot-shock delivered to their paws.

2.3 | Behavioural longitudinal study

To assess the severity of the behavioural dysregulation caused by the exposure to trauma, mice were subjected to a battery of behavioural tests 4 weeks after trauma (in consideration of Criterion F; DSM-V; American Psychiatric Association, 2013) (Figure 1a). The paradigms were chosen according to the symptomatic panel of PTSD (American Psychiatric Association, 2013). Increased startle response and hypervigilant behaviour (Criterion E; DSM-V; American Psychiatric Association, 2013), as well as marked physiological reactions to internal or external trauma-related stimuli (Criterion B; DSM-V; American Psychiatric Association, 2013), represent core symptoms of PTSD that were analysed by using the acoustic startle response (ASR) paradigm, and the contextual fear (CF) and fear generalization paradigms, respectively. Furthermore, we also explored mood disorders (Criterion D; DSM-V; American Psychiatric Association, 2013) and social impairments (Criterion G; DSM-V; American Psychiatric Association, 2013) that usually appear co-morbidly with PTSD. In this regard, we analysed anxiety behaviour with the holeboard test (HbT), anhedonia with the sucrose preference test (SPT) and social behaviour with the social interaction test (SIT). Paradigms were performed with at least 24 h in between each other. All behavioural tests were analysed with EthoVision XT 8.5 (Noldus; RRID:SCR_000441) unless differently stated.

- Acoustic startle response (ASR) (Sauerhöfer et al., 2012): The mouse was exposed to a set of 120 acoustic stimuli of four different intensities (75, 90, 105 and 115 dB) separated by random intervals (12–20 s) while inside a small cage within the startle station (Med Associates, USA). The order of the stimuli and the time between stimuli were randomised to avoid the habituation of the subject. The startle response, a proxy for hypervigilant behaviour, was measured using piezoelectric materials that registered the intensity of the startle response.
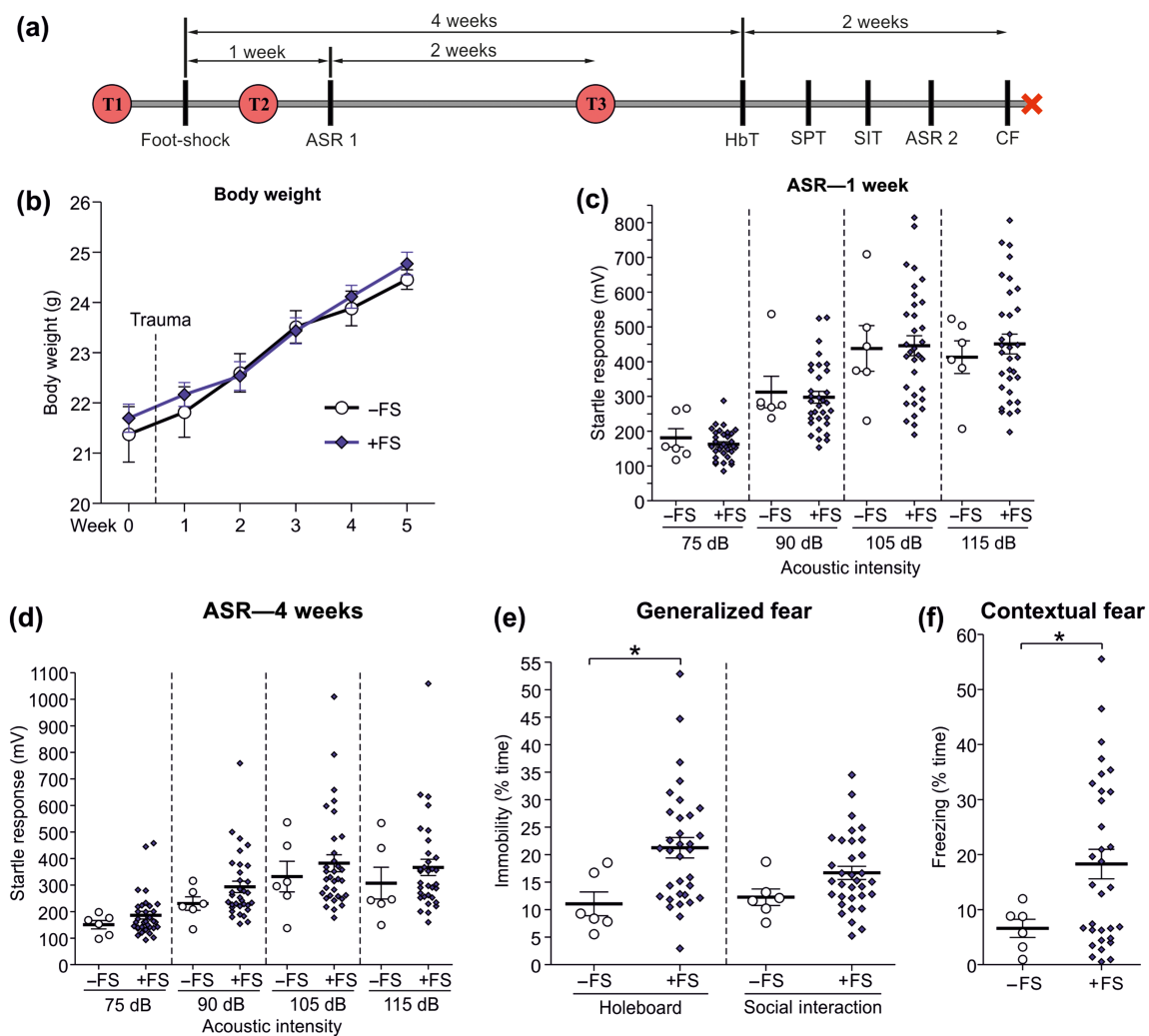
FIGURE 1 Experimental schedule, body weight and behaviour of core PTSD symptoms in control and trauma-exposed mice. (a) Experimental schedule to study long-term post-traumatic stress disorder-like behaviours and resilience in control ($-$FS; $n = 6$) and trauma-exposed mice ($+$FS; $n = 33$). ASR, acoustic startle response; CF, contextual fear; HbT, holeboard test; SIT, social interaction test; SPT, sucrose preference test. The red dots indicate time points for sample collection (blood and faeces). The red cross after CF indicates the time point for brain collection. (b) Body weight curve from experimental animals during the experiment. For both groups, body weight increased significantly with time. Data shown are means ± SEM. two-way ANOVA with repeated measures. (c) Scatter plot showing hypervigilant behaviour, as measured in the ASR, 1 week after trauma exposure. (d) Results of the second exposure to ASR, 4 weeks after the trauma. Data shown are individual values with means ± SEM. $^*P < 0.05$; two-way ANOVA with repeated measures. (e) The immobility of experimental subjects when exposed to new environments (in HbT and SIT) was used as a measure of fear generalization. (f) Measurement of the fear response (freezing) when exposed to the trauma context. Data shown are individual values with means ± SEM. $^*P < 0.05$; significantly different as indicated; unpaired two-tailed Student's t test

- Holeboard test (HbT) (Rey et al., 2012): The anxiety-like behaviour of the mouse was measured for 10 min in a squared arena (40 × 40 × 30 cm) with four equidistant holes in the centre. We measured the number of head dips (i.e., the mouse exploring the holes by introducing its head) and the latency to the first head dip as parameters of anxiety-like behaviour. The number of head dips was counted manually.

- Social interaction text (SIT) (Muir et al., 2018): The sociability of the trauma-exposed mouse was analysed by exposure to a squared arena (40 × 40 × 30 cm) for 5 min in two consecutive phases. During habituation phase, the arena contained an empty circular cage, whereas in the social phase, the same type of cage contained a mouse of the same sex and age. We measured the time that the mouse spent in the interaction area (8-cm radius around the cage), as well as the time the mouse interacted with the circular cage by using its nose. The sociability index was calculated as follows:

$$\text{Sociability index} = \frac{t\text{ in zone (social phase)} * 100}{t\text{ in zone (habituation)} + t\text{ in zone (social phase)}} - 50.$$

- Generalized fear (GF) (Asok et al., 2018): During the performance of the HbT and SIT, we observed that some mice showed behaviour consistent with the fear response in what should be neutral

environments. Thus, we decided to analyse the immobility time in these neutral environments to evaluate whether the subject displayed some form of fear generalization.

- Sucrose preference test (SPT) (Liu et al., 2018): Anhedonia was analysed by measuring the amount of sucrose water (1% w/v) that the mouse drank compared with normal tap water when presented with both options. The mouse was habituated to the presence of two different bottles in its cage for 2 days. Afterwards, one of the bottles was filled with sucrose water, and the weight of both bottles was measured for three consecutive days between 11:00 AM and 12:00 AM. The placement of the bottles was switched after every measurement to avoid habituation. We analysed the consumption of sucrose water and the preference index as a proxy for anhedonia. The preference index was calculated on the basis of the liquid consumption of each mouse as follows:

$$\text{Preference index} = \frac{\text{volume sucrose}}{\text{volume water} + \text{volume sucrose}} / \text{body weight}.$$

- Contextual fear (CF) (Shoji et al., 2014): In order to measure the strength of the memory to the trauma, the mouse was re-exposed to the trauma context for 10 min. During this time, the freezing behaviour of the mouse, that is, absence of movement except for that of breathing, was recorded and measured using custom software that analysed the amount of pixels that changed between video frames.

2.4 | Behavioural profiling

A mouse was classified as having a resilient or susceptible endophenotype depending on its individual behaviour in the different behavioural paradigms. The aim of the applied criteria was to include those trauma-exposed individuals with extreme responses across most of behavioural paradigms (i.e., >50%, meaning at least four out of seven behavioural domains). At the end, these extreme responders would then be categorized as resilient (R+) or susceptible (R−) endophenotypes. The following procedure was applied:

- Using the behaviour from the unexposed, non-stressed group (−FS) as reference, 'normal' behaviour was defined for each paradigm applied when falling within the 85% confidence interval (85% CI).
- Within the trauma-exposed group (+FS), each mouse was classified individually in each paradigm as a 'resilient' or 'susceptible' subphenotype depending on whether its behaviour fell within the range of 'normal' behaviour (within 85% CI) or outside of the 85% CI, respectively.
- The trauma-exposed mouse was finally categorized globally into the resilient or susceptible endophenotype, when it showed a consistent behaviour across the different behavioural paradigms of the longitudinal study, with the following criteria: The mouse was classified regarding a 'resilient' or 'susceptible' subphenotype in at least four out of the seven (i.e., >50%) of all behavioural domains. Furthermore, it was allowed that one classified behavioural subphenotype could belong to the opposite subphenotype in relation to the global categorization.

When a mouse displayed traits of both resilient and susceptible behaviour within the same paradigm, the mouse was then counted as 'unclassified' for that specific paradigm. We identified six R+ (18.8%) and four R− (12.5%) individuals within our trauma-exposed cohort using these criteria. We included two additional mice to the R− group (Mouse S5 and S6; see Table S1) in order to balance the number of replicates in both groups for the molecular characterization, as the behaviour of these mice also suggested strong R− features. A detailed list with the classification of R+ and R− mice for each paradigm can be found in Table S1.

2.5 | Sample collection

Using a lancet, blood was drawn from the facial vein and collected into 1-ml EDTA-coated tubes (KABE Labortechnik). Mice were immobilized during this procedure by gripping the loose skin behind the animal's neck. No anesthesia was used during the procedure as isoflurane, the drug of choice for sedation/anaesthesia, is known to interfere with plasma levels of endocannabinoids (Jarzimski et al., 2012; Schelling et al., 2006; Weis et al., 2010), as well as inducing amnesic effects (Dutton et al., 2002; Fidalgo et al., 2012) and cognitive impairments (Lin & Zuo, 2011; Zhang et al., 2017). These potential effects could have influenced the behavioural and molecular data we acquired. For every time point, four to five drops of blood were collected per mouse, and the animal was afterwards returned to its home cage. The blood was centrifuged ($\sim$10,000 × g, 10 min), and the plasma was collected and immediately frozen on dry ice.

Stool samples were collected on the same day as the blood was collected. Before the blood collection, the mouse was placed in an empty cage and left undisturbed. Then, the mouse was removed from the cage and prepared for blood collection once it had defecated at least two to three times, which usually took about 5–10 min. Faeces were collected with sterile tweezers and immediately frozen in dry ice. Both the tweezers and the empty box containing the mouse were thoroughly cleaned with ethanol between animals.

2.6 | Dual extraction of RNA and lipids from brain regions

The simultaneous extraction of RNA and lipids from the same sample was performed as described by Lerner et al. (2018). In short, mice were decapitated while under isoflurane anaesthesia. The brain was placed in chilled PBS and dissected. Brain regions of interest were visually identified and dissected with the help of a brain matrix (Ted Pella Inc). The dissected brain tissues were weighed and inserted into cold 2-ml Precellys tubes with RNase-free ceramic beads and a mix of

600 μl of RLT buffer from the RNeasy® mini kit (Qiagen, Germany) with 1% β-mercaptoethanol and 200 μl of chloroform. To this solution was added a mixture (10-μl) of internal standards for different lipid molecules (Avanti Polar Lipids, Inc.; Table S2). The samples were homogenized using a Precellys tissue homogeniser (1 cycle, 20 s, 6000 r.p.m.) (Bertin, France) and transferred to a new tube. After centrifugation of samples (10,000 x g for 3 minutes at 4°C), two phases were formed: an upper RNA-containing phase and a lower chloroform phase with the lipids. Each phase was then transferred to new tubes for further processing.

The upper phase was used for RNA extraction following the instructions of the RNeasy mini kit (Qiagen, Germany), including DNase I treatment for the removal of genomic DNA. Finally, total RNA from the sample was eluted in 30 μl of RNase-free water. The lower lipid-containing phase was mixed with 800 μl of methyl *tert*-butyl ether /methanol, in a 10:3 v/v proportion, and 250 μl of ice-cold 0.1% formic acid. Samples were vortexed for 30 min at 4°C and centrifuged afterwards for 15 min at 10,000 x g. The organic phase was removed and evaporated using a gentle stream of nitrogen. Samples were then reconstituted in 90-μl methanol, and 18 μl of this solution was mixed with 2 μl of water. For the analysis of endocannabinoids and polyunsaturated fatty acids, 27 μl of the final solution was evaporated once more and dissolved in 30 μl of acetonitrile mixed with water (1:1 v/v). A full list of the internal standards used for this experiment can be found in Table S2.

2.7 | cDNA generation and real-time quantitative PCR

The cDNA was generated from 1 μg of RNA using the High-Capacity cDNA Reverse Transcription Kit (Life Technologies, Germany). This kit uses random hexamers in order to reverse transcribe RNA strands in the sample. The resulting cDNA was diluted 1:12 in RNase-free water and stored at −80°C. The qPCR procedure was carried out by using Power SYBR Green PCR Master Mix (Life Technologies, Germany) and custom primers for a selection of genes (Table S3) in a QuantStudio 3 Real-Time PCR System (Life Technologies, Germany). Each PCR reaction mix consisted of 10-μl SYBR Green Master Mix, 8 μl sample, and 2 μl of a mix of the forward and reverse primers (each 5 μM).

2.8 | Lipidomic quantitative profiling from brain tissue

Targeted lipid profiling was invariably carried out in polarity switching using a 5500 QTrap triple-quadrupole linear ion trap mass spectrometer (RRID:SCR_020517) (AB SCIEX, Darmstadt, Germany), interfaced with an Agilent 1200 series LC system (RRID:SCR_018037) (degasser, pump and thermostated column compartment; Agilent, Waldbronn, Germany). The LC conditions were set as recently described (Lerner et al., 2019). Briefly, chromatographic separation of lipids was

achieved using a 2.5-μm C18 column, 100 × 2 mm (Phenomenex, CA, USA). For PL and sphingolipid analysis, the column was thermostated at 45°C and the mobile phase A consisted of methanol/water (1:1; v/v) containing 0.2% formic acid, 7.5-mM ammonium formate and 0.1% triethylamine, whereas the mobile phase B consisted of methanol/isopropanol (2:8; v/v) containing 0.2% formic acid, 7.5-mM ammonium formate and 0.1% triethylamine. The flow rate was 200 μl·min^{-1}. Gradient elution began at 40% B, was held for 3 min and was then linearly increased over 42 min to 90% B, then linearly increased to 99% B in 1 min, held there for 7 min and decreased over 2 min to 40% B. For analysis of endocannabinoids and polyunsaturated fatty acids, the mobile phase A consisted of 0.1% formic acid and the mobile phase B of 100% acetonitrile containing 0.1% formic acid. The flow rate was set to 300 μl·min^{-1}. Gradient elution began at 20% B, held so for 1 min, then linearly increased over 4 min to 50% B, maintained so for 7 min, linearly increased to 90% B over 1 min, held for 4 min and decreased over 0.5 min to 20% B. The column was then re-equilibrated with 20% B for 2.5 min.

Quantification of lipids was conducted via Analyst 1.6.2 software and MultiQuant 3.0 quantitation package (AB SCIEX, Darmstadt, Germany). The obtained values were normalised to the tissue weight. The complete list of lipids analysed in each brain region is specified in Table S4.

2.9 | Extraction of bacterial DNA from stool samples

To characterise the mouse gut microbiota, we used the QIAmp Fast DNA Stool mini kit (Sigma) following the manufacturer's instructions. In summary, one to three faeces were homogenised in InhibitEX buffer (Sigma) by vortexing. The homogenate was centrifuged at 10,000 x g for 1 min, and 600 μl of the supernatant was transferred to a tube containing 25 μl of proteinase K to digest any protein in the sample. Buffer AL (600 μl) was added to the mix, and a 10-min incubation at 70°C was performed to ensure the lysis of all cells and the denaturation of proteins. Afterwards, 600 μl of ethanol was added to the lysate and mixed. This mixture was then passed through a QIAamp column (Qiagen) and washed with different buffers (AW1 and AW2). The DNA was eluted using 200-μl nucleic acid-free water. Each sample was measured using NanoDrop to determine the concentration and purity of the DNA extraction.

2.10 | Library preparation and sequencing from stool samples

DNA samples were amplified via PCR using a primer combination (515F and 806bR) specific for the hypervariable region V4, found within the bacterial 16S ribosomal RNA (rRNA) gene sequences. The amplicons generated via PCR were then used for library preparation as per the manufacturer's instructions (Illumina, USA). Among other steps, two Illumina adapters were ligated to the sequences of interest

to provide a forward and backward reading frame (GGCTGACTGACT and ACAATTACCATA, respectively) and spiked with PhiX control v3 library (Illumina, USA) in order to balance the base composition and improve the quality of the run.

Libraries were then pooled and loaded in a flow cell to be processed in an Illumina MiSeq sequencer (RRID:SCR_016379). All 36 samples were sequenced in the same flow cell, which gave a yield of 20–30 million reads in total (including ∼25% of PhiX library). Pair-end reads were 300 nucleotides long, covering the whole 16S V4 region.

2.11 | ELISA

Corticosterone levels were measured from plasma samples by using the Corticosterone ELISA Kit (Cat. ADI-900-097; RRID:AB_2307314) (Enzo Life Sciences, Farmingdale, NY, USA). Samples were diluted prior to starting the experiment 1:40 following the instructions from the kit. Five different standards were prepared with final corticosterone concentrations of 20,000, 4000, 800, 160 and 32 pg·ml^{-1} in order to establish a standard curve. The ELISA was performed according to the manufacturer's instructions on a 96-well plate provided in the kit. The plate was measured in a FluoStar Galaxy photometer (BMG Labtech, Germany). All samples, standards and controls were performed in duplicate.

2.12 | Bioinformatic analysis of gut microbiome data

16S rRNA genomic sequencing data were processed using mothur v1.40.5 (RRID:SCR_011947). Briefly, reads were merged into contigs, and sequences with any ambiguous bases or homopolymers longer than eight bases were removed. Sequences were then aligned to the SILVA (RRID:SCR_006423) reference alignment, and chimeras were removed using VSEARCH. Taxonomy was assigned using the Greengenes database (RRID:SCR_002830). Sequences with identical taxonomy were grouped into operational taxonomic units (OTUs). Statistical analysis and visualization were then performed using the *phyloseq* R package v1.32 (RRID:SCR_013080). Alpha diversity was estimated by rarefying each sample to the smallest library size and calculating the diversity index (Chao1 and Shannon index). This procedure was repeated 1000 times, and the average over all runs was reported as the final diversity estimate. Beta diversity was calculated on the basis of Bray–Curtis dissimilarity and visualized using constrained analysis of principal coordinates (CAP). Changes in alpha diversity as well as taxonomic composition at the phylum level were evaluated using linear mixed-effects models calculated with lme4 v1.1-23. The significance of the fixed effects phenotype and time point was evaluated using the car package v3.0-8. Pairwise comparisons were performed with the emmeans package v1.4.8. Differential abundance analysis at the species level was performed with the DESeq2 package v1.28 (RRID:SCR_000154) with default settings.

Bacterial species were considered to be differentially abundant if the adjusted *P* value for the corresponding log2 fold change was below 0.1. *P* value adjustment was facilitated with the Benjamini–Hochberg method. Outlier values in the analysis of relative bacterial abundance at the phylum level between R+ and R− animals were detected by inspecting Q–Q plots of residuals of the fitted linear mixed-effects model using the qqPlot function from the car R package and calculating Cook's distance with the CookD function from the predictmeans R package. Values marked as outliers in the Q–Q and Cook's distance plots were removed from the statistical analysis. Excluded outlier values are indicated in the figure legend and colour coded on the respective panel in Figure 6.

2.13 | Statistical analysis of behavioural, lipidomic, ELISA and real-time quantitative PCR data

Continuous variables were graphically represented as individual values with means ± SEM. No statistical analysis was performed with groups with *n* < 5. The declared group size is the number of independent values, which were used for statistical analysis. Unless otherwise stated, two groups were compared statistically with an unpaired *t* test with Welch's correction or a non-parametric Mann–Whitney test. More than two groups were analysed using either one-way ANOVA or two-way ANOVA with repeated measures in cases where the variables were measured at multiple time points. The assumption that variances are homogeneous was tested using InVivoStat (IVS) by generating a scatterplot representing the standardised residuals against the predicted values. This analysis was complemented with the Bartlett's and Lavene's test to ensure that the assumption was not violated when we performed ANOVA. Post hoc tests were conducted only if the *F* value of the ANOVA analysis achieved statistical significance. Statistical analysis was performed with GraphPad Prism v5.0 (RRID:SCR_002798) and InVivoStat (IVS). *P* values were two tailed, and differences were considered statistically significant if the *P* value was below 0.05. The data and statistical analysis comply with the recommendations of the *British Journal of Pharmacology* on experimental design and analysis in pharmacology (Curtis et al., 2018).

Regarding the real-time quantitative PCR (RT-qPCR) data, the relative expression of each gene was calculated by normalizing the Ct values of each sample to the respective Ct values from a housekeeping gene (GAPDH) and transformed into a normal distribution according to the delta–delta Ct (ΔΔCt) method. The average value of the biological replicates from the R+ group was used as a reference in order to present the results relative to the R+ group.

2.14 | Multiomics integrative analysis

We employed sparse partial least squares discriminant analysis (sPLS-DA) as implemented in the mixOmics R package v6.12.2 (RRID:SCR_016889) in order to identify features with high discriminative power of the susceptible or resilient phenotype by

integrating data across the different omics layers (lipidome, microbiome and transcriptome). We used fivefold cross-validation with maximum distance to select the optimal number of components and variables to keep in the sPLS-DA model. In order to reduce the impact of sampling error, we repeated the parameter tuning step 50 times with distinct seed values. The average number of variables per component across the 50 iterations was used for the final model. The relationship between the selected features was evaluated by calculating the Pearson correlation coefficient. Significant correlations were used to construct an interaction network, which was visualized in Cytoscape v3.8.1 (RRID:SCR_003032) with the MetScape plugin v3.1.3 (RRID:SCR_014687).

2.15 | Materials

Isoflurane was supplied by Piramal Critical Care B.V. (Voorschoten, Netherlands).

2.16 | Nomenclature of targets and Ligands

Key protein targets and ligands in this article are hyperlinked to corresponding entries in the IUPHAR/BPS Guide to PHARMACOLOGY http://www.guidetopharmacology.org and are permanently archived in the Concise Guide to PHARMACOLOGY 2021/22 (Alexander, Christopoulos, et al., 2021; Alexander, Cidlowski, et al., 2021; Alexander, Fabbro, et al., 2021; Alexander, Kelly, et al., 2021).

3 | RESULTS

3.1 | Long-term behavioural dysregulations induced by trauma allow the classification of resilient and susceptible individuals

In order to assess the effects of the exposure to trauma (foot-shock, FS) on behavioural responses, we performed the ASR 1 week after trauma, followed by a longitudinal behavioural study 4 weeks after the FS (Figure 1a). There were no differences in body weight between control ($-$FS, $n = 6$) and trauma-exposed ($+$FS, $n = 33$) mice (Figure 1b) at any time point measured. However, food consumption was not measured during the study. The battery of tests consisted of paradigms related to symptoms that are considered central in PTSD, such as increased hypervigilance and startle, measured in the ASR (Figure 1c,d), a generalization of fear (GF), measured as immobility in the HbT and the SIT (Figure 1e), and a persistent trauma memory, measured as freezing in the trauma context (Figure 1f). Furthermore, we analysed maladaptive behaviours commonly found in PTSD patients by including additional behavioural domains (Figure S1), such as anxiety (measured in the HbT), anhedonia as a proxy of depressive-like behaviour (measured in the SPT) and sociability (measured in the SIT). We observed significant differences between the $-$FS and $+$FS

groups in both GF and CF (Figure 1e,f), as well as in anxiety behaviour (Figure S1a). These trauma-induced maladaptive behaviours were stable for at least 4 weeks after trauma. Furthermore, our trauma model induced a large dispersion of the individual behaviour within the $+$FS group. Such a heterogeneous behavioural response is also typically observed in human cohorts of PTSD patients and is a prerequisite for stratifying different endophenotypes within the $+$FS group.

Thus, we profiled $+$FS animals based on their individual behavioural responses across the longitudinal study into resilient (R$+$), if they consistently showed behaviour similar to the control group ($-$FS), or susceptible (R$-$), if they showed maladaptive behaviour (see Section 2 for more details of the classification). Our profiling method identified six R$+$ (18.75%) and six R$-$ (18.75%) mice, whereas the majority of animals (62.5%) showed a so-called undefined phenotype with mixed traits of resilience and susceptibility (Figure 2a). We observed the expected significant increase of body weight over time in the animals, but we could not detect an effect of the phenotype (Figure 2b). We also found significant behavioural differences between the R$-$ group and both R$+$ and $-$FS groups in the ASR exposures 1 and 4 weeks after trauma (Figure 2c,d), and anxiety-like behaviour in the HbT (Figure S2a). Furthermore, there were significant differences between R$-$ and $-$FS animals, but not between R$-$ and R$+$ animals, in fear generalization (Figure 2e), CF (Figure 2f) and the latency to the first head dip in the HbT (Figure S2b). Interestingly, we observed increased social behaviour in R$+$ animals compared with the $-$FS group in the SIT (Figure S2c), but not in comparison with R$-$ mice. We did not observe significant differences between groups in sucrose preference (anhedonia) (Figure S2d,e). Taken together, these data indicate that the single-trauma PTSD-like mouse model induced a highly individualized behavioural response, as well as long-term maladaptive behaviour. When combined with behavioural profiling, we were able to reveal within the $+$FS group two distinct subgroups that are behaviourally different from each other and can be categorized into R$+$ (resilient) and R$-$ (susceptible) endophenotypes.

3.2 | Long-term differences in phospholipid levels in dorsal hippocampal subregions

After the behavioural profiling and categorization, we analysed different molecular domains to understand possible underlying mechanisms for the presence of the R$+$ and R$-$ endophenotypes. Given the essential roles of lipids in neural functions, we analysed various lipid molecules from the dorsal hippocampus (Figure 3) and PFC of R$+$ and R$-$ mice (Table S4), with a particular focus on phospholipids (Figure 3). Although no significant differences were observed in the PFC, several alterations were revealed in the hippocampus. We analysed the cornus ammonis (CA) (Figure 3a–f) and the dentate gyrus (DG) (Figure 3g–j) from the dorsal hippocampus separately. Six weeks after the trauma, we observed increased levels of the phospholipids, **phosphatidylethanolamine** and phosphatidylcholine, in the dorsal CA of R$-$ mice, both reported to be stress-inducible (Faria et al., 2014). **Sphingosine-1-phosphate** and sphingomyelin, both known to
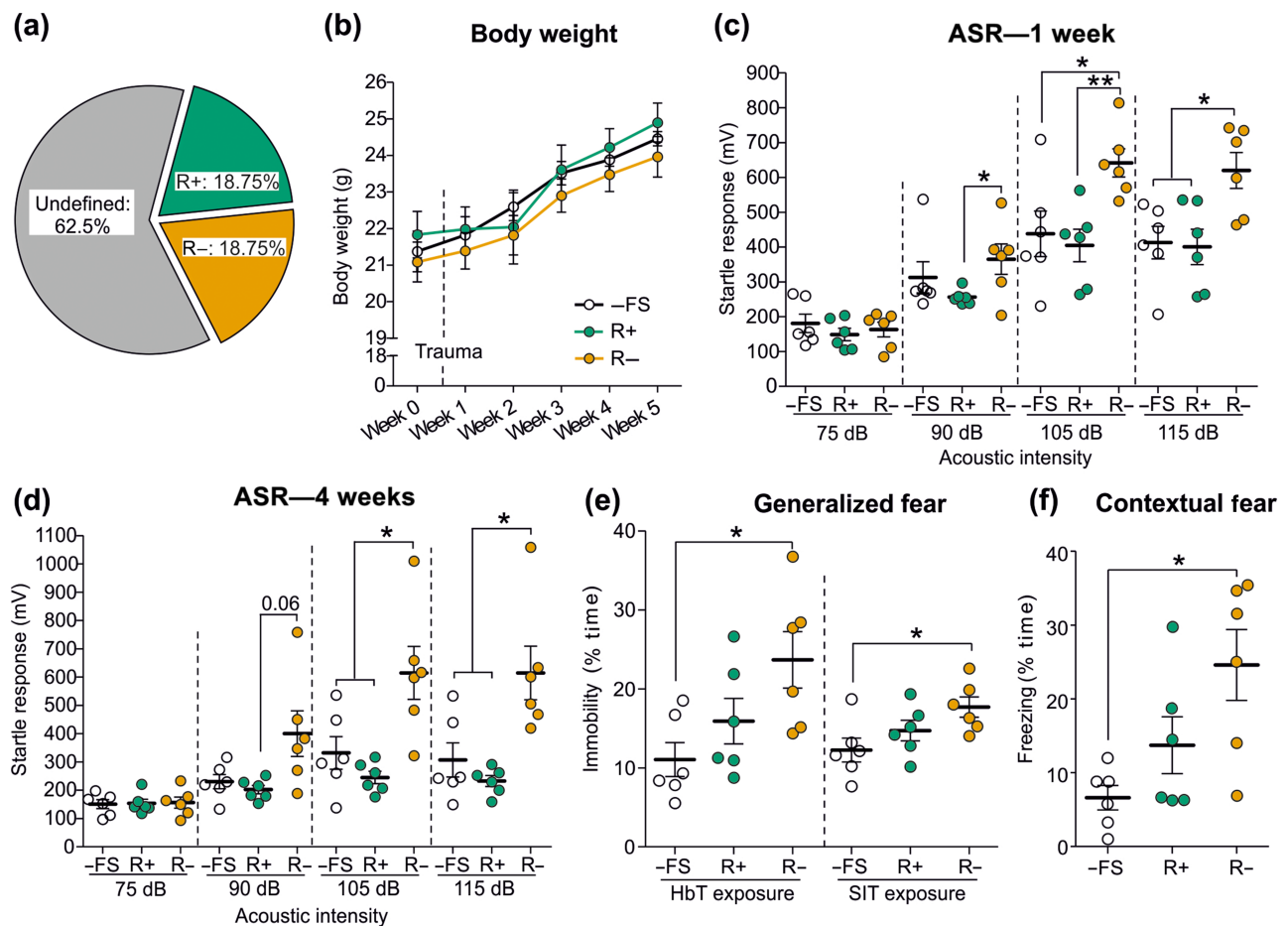
FIGURE 2 Results of behavioural profiling, body weight and behaviour of core PTSD symptoms in resilient and susceptible mice. (a) Percentage of trauma-exposed mice that matched the criteria for the resilient (R+, $n = 6$) and susceptible (R−, $n = 6$) phenotypes after behavioural profiling. (b) Body weight curve from R+ and R− mice during the experiment compared with controls ($n = 6$). There was a significant effect of time for all groups. Data shown are means ± SEM. (c, d). Hypervigilant behaviour of R+ and R− mice as measured by acoustic startle response (ASR) (c) 1 week after and (d) 4 weeks after the trauma. There was a significant effect of phenotype at 1 week and also at 4 weeks. Data shown are individual values with means ± SEM. $^*P < 0.05$; two-way ANOVA with repeated measures. (e) Percentage of immobility time of R+ and R− mice when exposed to novel environments, during holeboard test (HbT) and social interaction test (SIT). (f) Strength of the fear memory in R+ and R− mice in the trauma context. Data shown are individual values with means ± SEM. $^*P < 0.05$; unpaired two-tailed Student's t test

promote neural homeostasis (Grassi et al., 2019), were more abundant in R+ samples of the dorsal CA region. The phospholipids **phosphatidylserine** and phosphatidylglycerol were also more abundant in R− samples in the dorsal CA but were decreased in the dorsal DG. Furthermore, **lysophosphatidylinositol** was decreased in DG of R− mice. Interestingly, all lipids with alterations in the dorsal DG showed reduced levels. Altogether, these observations suggest that the effect of trauma on brain phospholipid levels is highly dependent on the brain region examined, and that the hippocampus was particularly affected by stress.

3.3 | Long-term differences in the gene expression profiles of R+ and R− mice

Next, we performed a gene expression analysis in the dorsal hippocampus and the PFC by RT-qPCR of selected genes based on their roles in brain function and stress-related disorders (Tables S3 and S5). We observed increased mRNA levels of several genes in R− individuals as compared with R+ in the PFC, but reduced gene expression in the dorsal hippocampus of the same individuals (Figure 4), and with one alteration found in the dorsal DG, where the gene for **cortistatin, Cort**, was increased in R+ mice (Table S3). Among these differentially expressed genes, we found those for the glucocorticoid receptor, *Nr3c1* (GR; Figure 4a) and for the CRH₂ receptor, *CRHR2* (Figure 4b), both involved in regulating the stress response. We also observed in the R− group increased levels of the gene for acid sphingomyelinase, *Smpd1* (ASM; Figure 4c), an enzyme whose inhibition was shown to improve fear memory extinction (Huston et al., 2016), Figure 4d), involved in behavioural regulation. Additionally, the genes for the enzyme responsible for synthesizing **GABA**, **glutamic acid decarboxylase 2, Gad2**, and for an important epigenetic regulator of transcription, **CREB-binding protein, Crebbp**, were also found to be increased in R− mice compared with the R+ group (Figure 4e,f, respectively). Interestingly, we found
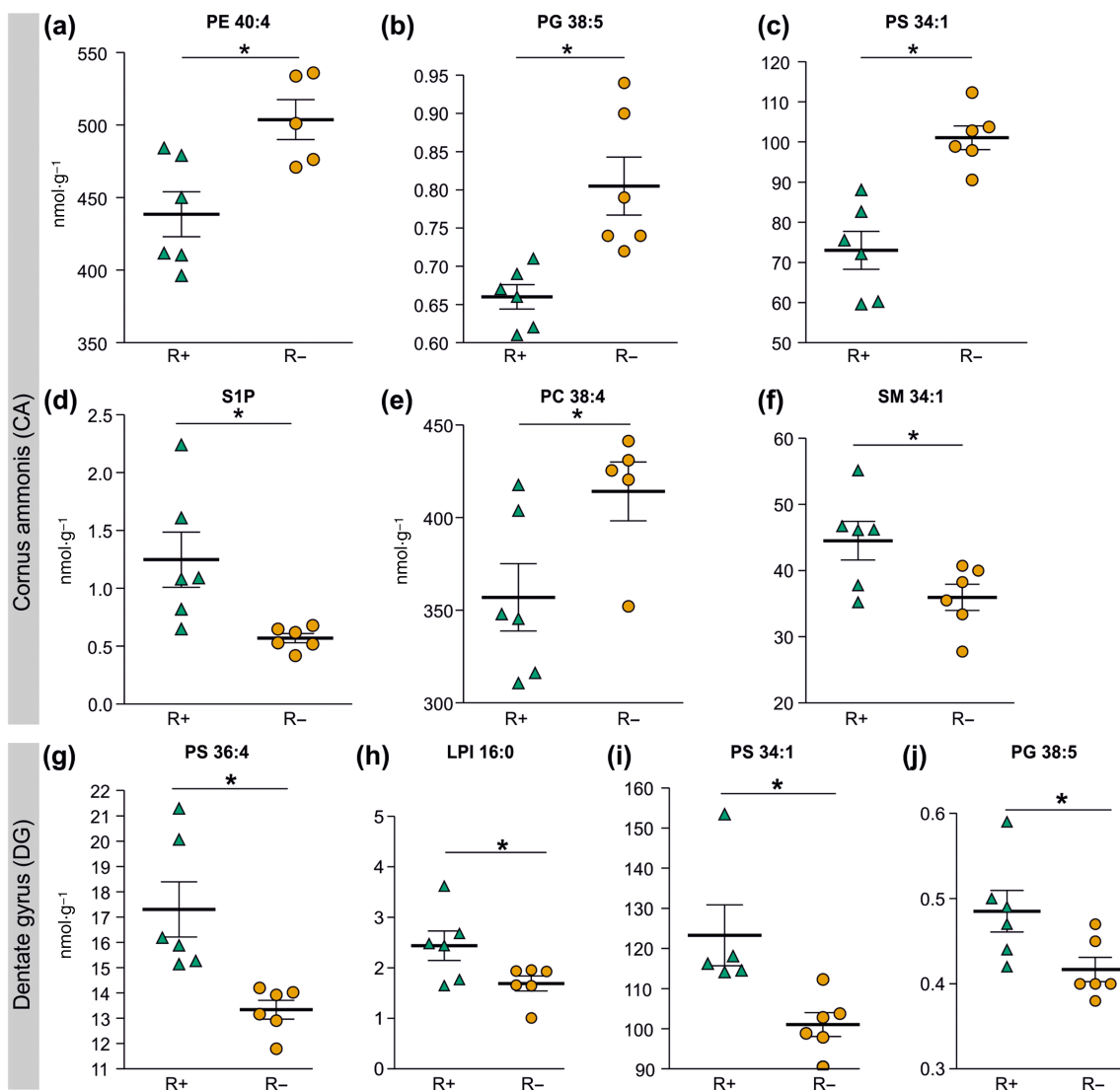
FIGURE 3 Phospholipid levels in the dorsal hippocampus of resilient and susceptible mice. Lipid levels were measured 6 weeks after the traumatic experience in resilient (R+, $n = 6$) and susceptible (R−, $n = 6$) mice. The numbers by the molecular species indicate the number of carbon atoms and of double bonds, respectively. In cornus ammonis (CA): (a) phosphatidylethanolamine (PE) 40:4, (b) phosphatidylglycerol (PG) 38:5, (c) phosphatidylserine (PS) 34:1, (d) sphingosine-1-phosphate (S1P), (e) phosphatidylcholine (PC) 38:4 and (f) sphingomyelin (SM) 34:1. In dentate gyrus (DG): (g) PS 36:4, (h) lysophosphatidylinositol (LPI) 16:0, (i) PS 34:1 and (j) PG 38:5. Data shown are means ± SEM. $^*P < 0.05$, significantly different as indicated; unpaired two-tailed Student's t test

components of the ECS with a lower relative expression in R− animals when compared with the R+ group in the dorsal hippocampal subregions. Both **cannabinoid receptors**, CB$_1$ (Figure 4g) and **CB$_2$** (Figure 4h), showed reduced mRNA levels in R− animals in the dorsal CA, although only the differences for CB$_2$ receptors were statistically significant. The genes for the enzymes **N-acylphosphatidylethanolamine-phospholipase D, Napepld** (Figure 4i) and **fatty acid amide hydrolase, Faah** (Figure 4j), responsible for the synthesis and degradation of **anandamide** (AEA), respectively, and **diacylglycerol lipase α, Dagla** (Figure 4k), which degrades **2-arachidonoyl glycerol (2-AG)**, also had reduced relative expression in the dorsal CA region of R− individuals. On the other hand, we could not observe significant differences for any component of the ECS in the dorsal DG, although CB$_2$ receptors showed a trend towards

reduced expression in R− animals, compared with R+ mice (Figure 4l). These results highlight a wide range of dysregulated processes in the PFC, such as GABAergic transmission, sphingolipid metabolism, neuropeptide signalling and epigenetic modulation, as well as the dysregulation of the ECS in the dorsal subregions of the hippocampus.

3.4 | Plasma measurements of endocannabinoids and corticosterone in trauma-exposed mice

Next, we measured the concentration of two endocannabinoids, AEA (Figure 5a,b) and 2-AG (Figure 5c,d) in the plasma. We also measured the plasma levels of **arachidonic acid**, palmitoylethanolamide and **oleoylethanolamide**, lipids that are involved in endocannabinoid
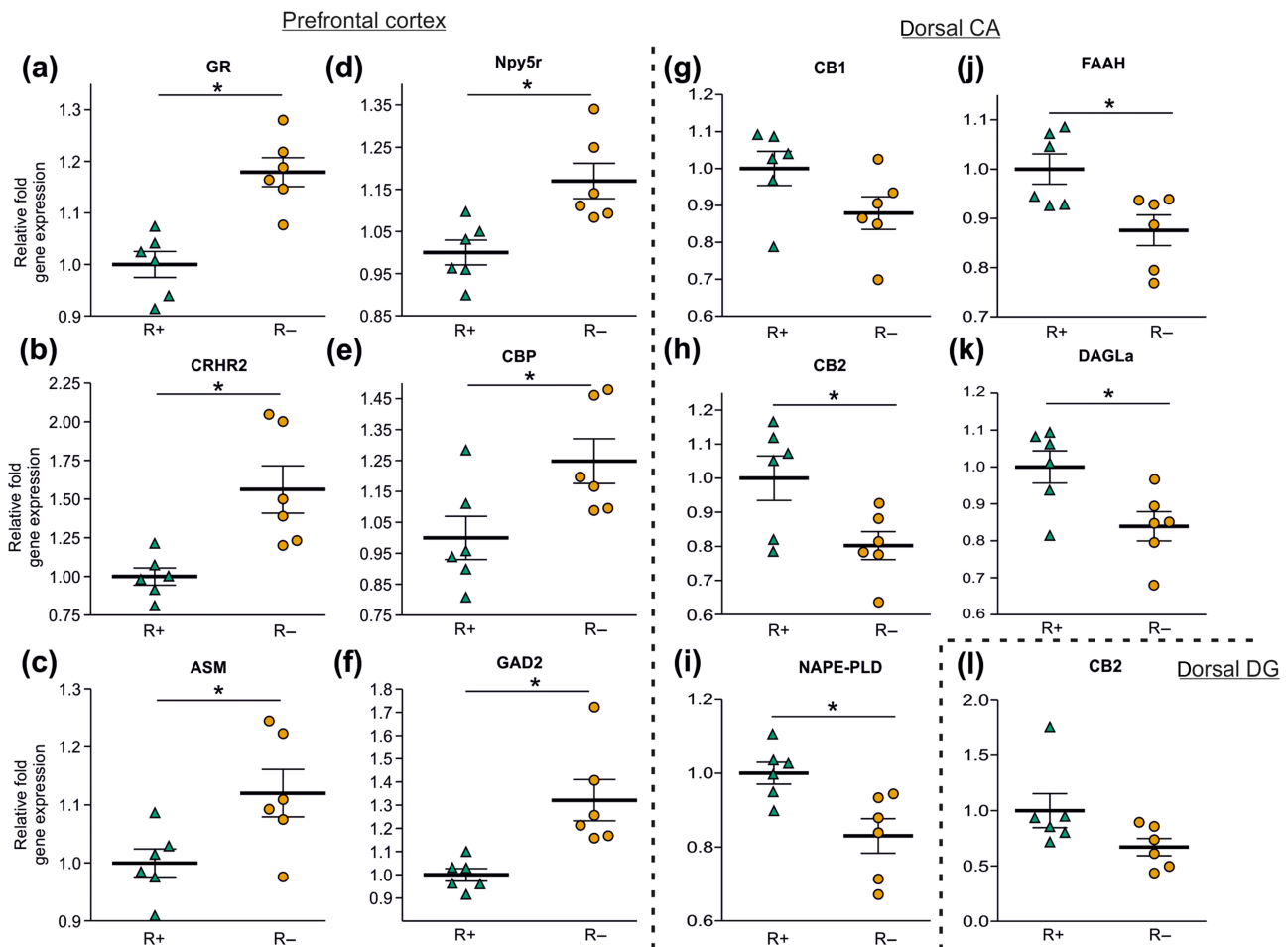
FIGURE 4 Relative gene expression in the prefrontal cortex. Expression of genes of interest in the prefrontal cortex of resilient (R+) and susceptible (R−) individuals was determined by real-time quantitative PCR. Genes were selected on the basis of their relevance to stress-related disorders and neural functions. (a) Glucocorticoid receptor (GR). (b) Corticotropin-releasing hormone receptor 2 (CRHR2). (c) Acid sphingomyelinase (ASM). (d) Y_5 receptor (Npy5r). (e) CREB-binding protein (CBP). (f) Glutamic acid decarboxylase 2 (GAD2). (g) CB_1 receptor (CB1). (h) CB_2 receptor (CB2) in the dorsal CA region. (i) N-acylphosphatidylethanolamine-phospholipase D (NAPE-PLD). (j) Fatty acid amide hydrolase (FAAH). (k) Diacylglycerol lipase α, (DAGLa). (l) CB_2 receptor (CB2), in the dorsal DG region. Data shown are individual values with means ± SEM. $^*P < 0.05$; significantly different as indicated; unpaired two-tailed Student's t test

metabolism or are related to endocannabinoids (Figure S3), as well as the stress hormone corticosterone (Figure S4). The blood samples were taken 1 week before (T1), 1 week after (T2) and 3 weeks after (T3) the trauma exposure (see Figure 1a). Moreover, we calculated the ratio between AEA and 2-AG (Figure 5e,f), as this value could potentially give information on the balance of the two major endocannabinoids. The levels of AEA, 2-AG and palmitoylethanolamide significantly increased over time when comparing −FS and +FS mice. However, the main effect of time was only significant for 2-AG and palmitoylethanolamide after behavioural profiling (i.e., for R+ compared with R− mice). In contrast, the ratio between AEA and 2-AG remained unchanged. Moreover, we did not observe any differences between control and +FS mice (Figure 5a,c,e) nor between the R+ and R− groups (Figure 5b,d,f) at any time point. The levels of arachidonic acid, palmitoylethanolamide and oleoylethanolamide remained relatively constant across the different time points and without differences between any of the experimental groups (Figure S3). Lastly, we

measured the plasma levels of corticosterone at the same three time points (Figure S4). We did not find any significant differences between the R+ and R− phenotypes nor across the different time points. However, a trend could be observed at T2 where R− mice showed a slight increase in corticosterone levels when compared with the R+ animals. In summary, we observed a significant effect of time in endocannabinoid levels (AEA and 2-AG) and in palmitoylethanolamide, but we did not observe statistical differences between the different groups analysed (i.e., −FS vs. +FS and R+ vs. R−) either before or after the traumatic experience.

3.5 | Characterization of the gut microbial community in R+ and R− phenotypes

The gut microbiome is gaining relevance in the research of stress-related disorders due to its influence on the immune system, the
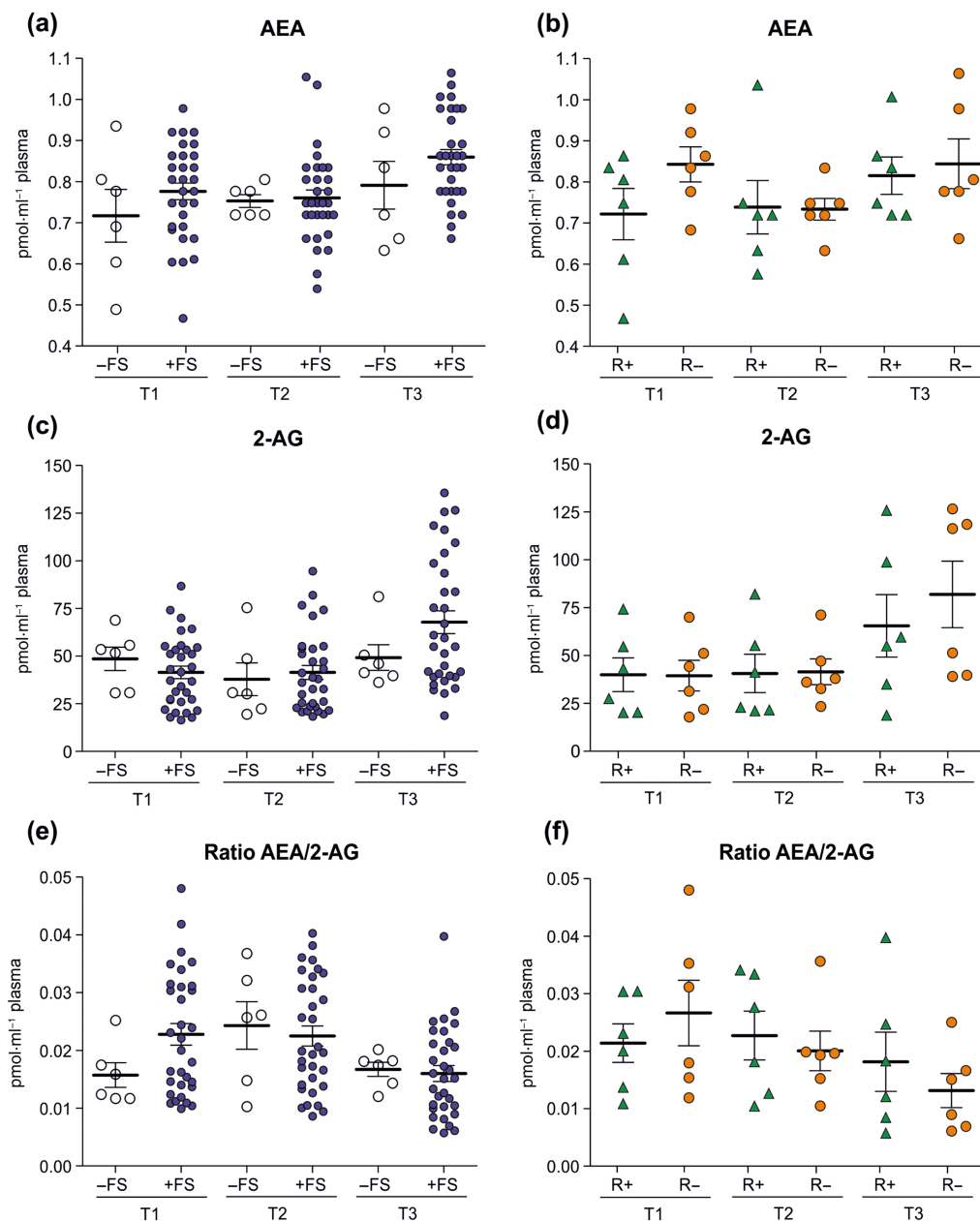
FIGURE 5 Plasma endocannabinoid levels and their ratios before and after the trauma. Circulating anandamide (AEA) and 2-arachidonoylglycerol (2-AG) levels in the plasma were determined 3 days before the trauma (T1), 1 week after the trauma (T2) and 3 weeks after the trauma (T3). (a) Circulating levels of AEA in control (−FS) and trauma-exposed mice (+FS). There was a significant effect of time for both groups. (b) AEA levels in blood in resilient (R+) and susceptible (R−) mice, showed no change over the experimental time. (c) Circulating levels of 2-AG in −FS and +FS mice. There was a significant effect of time for the +FS mice. (d) 2-AG levels in R+ and R− mice. There was a significant effect of time for both groups. (e) Ratio between AEA/2-AG levels in −FS and +FS mice. (f) AEA/2-AG ratio in R+ and R− mice. Data shown are individual values with means ± SEM

inflammatory state and brain processes including the HPA axis and behaviour. We analysed the composition of the gut microbiota in R+ and R− mice, 1 week before (T1) as well as 1 week (T2) and 3 weeks (T3) after trauma exposure. We did not observe differences in the number of distinct bacterial phylotypes as indicated by the Chao1 index (Figure 6a). However, susceptible mice were associated with a significantly higher Shannon index at baseline (Figure 6b). Exposure to trauma was followed by a significant reduction of alpha diversity in

both groups. The Shannon index was significantly reduced at T3 compared with T1 and T2 in resilient mice, whereas the difference was only significant at T3, relative to T1, in susceptible mice. Furthermore, constrained ordination analysis revealed that beta diversity significantly differed between the two phenotypes, whereas the effect of time was not significant (Figure 6c). We also detected shifts in the relative abundance of the major phyla of commensal gut bacteria, Bacteroidetes and Firmicutes. Interestingly, the proportion of Bacteroidetes
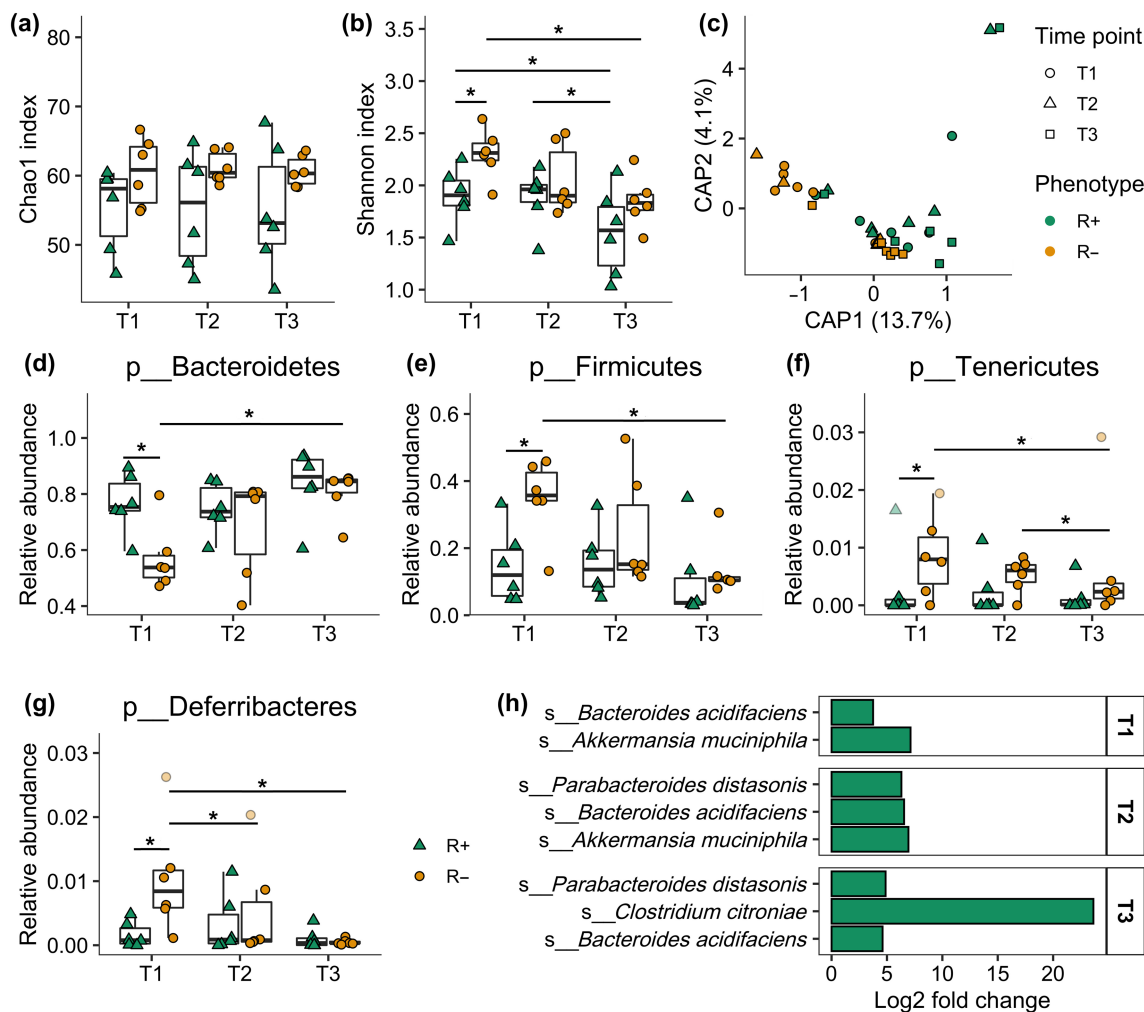
FIGURE 6   Gut commensal microbiota diversity and composition in resilient and susceptible mice before and after the trauma. The gut microbiota from resilient (R+) and susceptible (R−) mice was analysed at three different time points: 1 week before the trauma (T1), as well as 1 and 3 weeks after the trauma (T2 and T3). (a) Chao1 index corresponding to the total number of phyla detected as an estimate of alpha diversity. (b) Alpha diversity was complemented with the Shannon index, which also includes the evenness of the different phyla that were found. (c) The differences in beta diversity were evaluated using constrained analysis of principal coordinates (CAP). The impact of experimental factors on the ordination results was examined statistically with non-parametric permutational ANOVA. There was a significant effect of phenotype. (d–g) Box plots showing changes in the relative abundance of four bacterial phyla detected in the gut microbiome of R+ and R− individuals. Three outlier values in (f) and two outlier values in (g) are indicated with lighter colours. These values were removed from statistical analysis. (h) Differences in microbiota composition at the species level were investigated by estimating log2-fold changes of bacterial abundance. Positive log2-fold changes (adjusted P value <0.1) indicate species with a significantly higher abundance in R+ mice. $^*P < 0.05$; significantly different as indicated; differences in alpha diversity and phyla abundance between phenotypes and different time points were statistically compared with linear mixed-effects models followed by Tukey-adjusted pairwise comparisons

was significantly higher in resilient mice compared with the susceptible group (Figure 6d), whereas the opposite effect was present for Firmicutes. Two other bacterial phyla, Tenericutes and Deferribacteres, exhibited significantly increased abundance in R+ animals 1 week before trauma (Figure 6f,g). Such differences in the baseline composition of intestinal microbiota prior to trauma exposure could be indicative of certain predispositions to stress. It is noteworthy to mention that we observed shifts in the relative abundance of these phyla following trauma exposure, only in susceptible mice. Specifically, the proportion of Bacteroidetes significantly increased following the traumatic event, whereas the abundance of Firmicutes, Tenericutes

and Deferribacteres was significantly reduced. These longitudinal changes of the phylum composition in R− animals abolished the differences to R+ mice observed at baseline. Thus, it would be interesting to investigate further if the resilient phenotype is associated with a more stable gut bacterial composition. At the species level, we detected four bacterial phylotypes, which were all associated with a significantly increased abundance in R+ animals. *Bacteroides acidifaciens* was up-regulated in R+ mice at all three time points. In contrast, *Akkermansia muciniphila* demonstrated a significantly increased growth at T1 and T2, *Parabacteroides distasonis* at T2 as well as T3, and *Clostridium citroniae* at T3 only.

3.6 | Distinct multiomics signatures of R+ and R− individuals

To investigate whether the resilient and susceptible mice differ in their overall omics signatures, we performed a multiomics-integration analysis (Bersanelli et al., 2016; Ruffini et al., 2020). Here, we employed the sPLS-DA multivariate technique to integrate data from the three molecular domains investigated in our study: lipidome, transcriptome and microbiome. Resilient and susceptible mice formed two distinct clusters as indicated by non-overlapping 95% confidence ellipses (Figure 7a), which points to significant differences in the multivariate pattern of both phenotypes. The stress reactivity of resilient and susceptible mice was captured by the first sPLS-DA component with higher scores indicating resilient behaviour. The most critical molecular features that explained the separation of R+ and R− mice are shown in Figure 7b. This analysis highlighted that stress-related
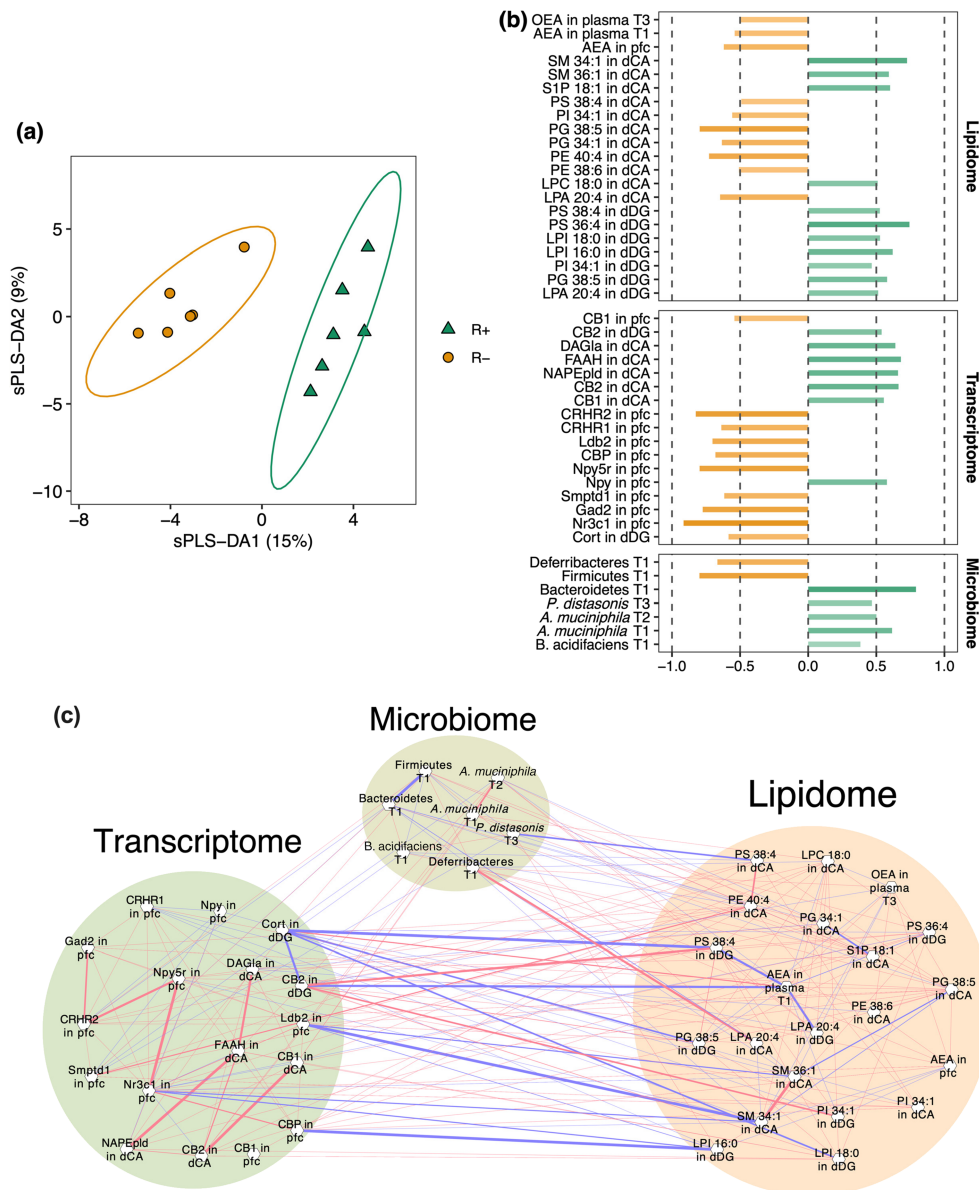

FIGURE 7 Distinct omics signatures in resilient and susceptible mice. Differences in the multivariate omics pattern were evaluated by integrating lipidome, transcriptome and microbiome data using sparse partial least squares discriminant analysis (sPLS-DA). (a) Resilient (R+) and susceptible (R−) animals were separated in reduced space along the first multivariate dimension. (b) Important features explaining the differences between R+ and R− mice. Variables coloured green are positively correlated with the resilient phenotype, and variables coloured orange are positively associated with the susceptible phenotype. (c) The correlation network of important omics features reveals statistically significant interactions within and between the three omics layers. Positive correlations are coloured red, and negative correlations are coloured blue. The line thickness is proportional to the magnitude of correlation. *Ldb2, LIM domain binding 2*; LPA, lysophosphatidic acid; LPC, lysophosphatidylcholine. LPI, lysophatidylinositol; NPY, neuropeptide Y; OEA, oleoylethanolamide; PC, phosphatidylcholine; PE, phosphatidylethanolamine; PG, phosphatidylglycerol; PI, phosphatidylinositol; PS, phosphatidylserine; SM, sphingomyelin; S1P, sphingosine-1-phosphate

changes in the lipidome were mainly limited to the hippocampus with a region-specific difference between dorsal CA and dorsal DG. Furthermore, expression levels of components of the ECS were mostly increased in the dorsal CA of R+ mice. In contrast, most of the remaining genes investigated were associated with an increased expression in the PFC of R− animals. Correlation network analysis revealed multiple associations of discriminative features within the different omics layers, but importantly, numerous strong interactions could also be observed across the different layers (Figure 7c). For instance, *Cortistatin* expression in the dorsal DG was significantly negatively correlated with the levels of the lipids, phosphatidyl serine 38:4, phosphatidyl glycerol 38:5 and lysophosphatidylinositol 18:0 in the same region. Furthermore, increased expression of *Crebbp* in the PFC was associated with reduced levels of lysophosphatidylinositol 16:0 in the DG region. In contrast, concentrations of phosphatidylethanolamine 40:4 in the dorsal CA were positively correlated with mRNA levels of *Smptd1* in the PFC. Notably, expression levels of the mRNA for CB$_2$ receptors in the dorsal DG exhibited a strong positive correlation with phosphatidylinositol 34:1 and phosphatidylserine 38:4 in the same region, while also being negatively correlated with circulating levels of AEA at the pretrauma time point. Interestingly, we detected a higher number of significant correlations for microbiome features with lipidome variables than with the transcriptome layer.

4 | DISCUSSION

Stress-related disorders pose a challenge to be studied, as they are influenced by very individual factors, such as past experiences or gender, and the stressor itself. Therefore, it has been difficult to mimic the human pathology using animal models, in a robust manner. PTSD is especially challenging due to the heterogeneity in its symptomatology, the high prevalence of co-morbid symptoms and individual differences among human patients. Additionally, research bias, for example, studying only the average group response, has led to poor translatability of the findings (Richter-Levin et al., 2019), which in turn has complicated the prognosis and treatment of these patients.

In this study, we used a single-trauma model able to induce a range of long-term maladaptive behaviours. Furthermore, the individual responses of trauma-exposed mice scatter widely, which resembles observations from human PTSD patients and provides a substrate to study different phenotypes within the trauma-exposed group. The behavioural profiling of these animals revealed two subgroups of mice, one that consistently showed resilience to trauma (R+), that is, they behave similarly to the non-stressed group, and the other a PTSD-like phenotype (R−). The resulting R- group showed behaviours indicative of PTSD, such as hyperarousal (tested by ASR) and maladaptive fear memories, as well in anxiety-like behaviour. Interestingly, a previous study found that the fear response and arousal state of individuals exposed to trauma could be used to predict susceptibility to PTSD-like phenotypes (Jeong et al., 2020; Torrisi et al., 2021). It is also important to note that only male mice were used in this study. As the

psychological perception of stress differs between males and females (Kokras & Dalla, 2014), this might generate a bias not only on the behavioural data but potentially also on the data from the different molecular domains analysed. Therefore, this limitation should be considered before extrapolating the results of this study. Moreover, the relatively low number of animals classified as R+ ($n = 6$) and R− ($n = 6$) and their intrinsic heterogeneity might mask molecular differences that would appear when studying larger cohorts of mice.

Given the relevance of the ECS during the stress response, we measured circulating levels of endocannabinoids during the period before and following trauma exposure. Previous studies had shown an effect of stress on the ECS and circulating endocannabinoid levels (Hillard, 2018), with 2-AG increasing after acute stress exposure, with no significant changes in AEA levels (Hill et al., 2009). We were only able to see a significant effect of time in the circulating levels of endocannabinoids and related molecules, but no difference between groups. The lack of statistical differences between groups could be due to differences in the type and severity of the trauma and technical differences between the individual scientific studies. Furthermore, a much larger number of trauma-exposed mice would be necessary to increase the numbers of R+ and R− mice required to uncover significant differences, as endocannabinoid measurements generally need large sample sizes (Buczynski & Parsons, 2010). Moreover, the lack of significant differences in corticosterone levels could be due to the same low sample size, but also due to the timing of sample collection, as samples were not collected immediately after trauma exposure. Thus, it is not possible to exclude a dysregulation of the HPA axis caused by the trauma.

We also examined the composition of the gut microbiome during the period before and following trauma exposure, as commensal microbiota has the potential to alter CNS functions, including behaviour. Germ-free mice showed reduced anxiety (Huo et al., 2017) and freezing after cued fear conditioning (Hoban et al., 2018). In addition, there is evidence of a direct communication between the microbiota and the host on the molecular level (Hewel et al., 2019; Liu et al., 2016). In our study, exposure to trauma was associated with a significant reduction in alpha diversity irrespective of the phenotype as measured by the Shannon index. This observation is in agreement with previously described dysbiosis-inducing effects of stress on gut microbiota (Reber et al., 2016). We also observed a strong effect on the phenotype's beta diversity, which additionally hinted at the R− group being slightly different from R+ animals at pretrauma time point (T1). An analysis of the different taxa that inhabit the gut of R+ and R− subjects revealed increased abundance of *A. muciniphila*, a bacterium considered as a biomarker for a functional intestine, in R+ animals at T1 and T2. Furthermore, previous studies have shown that *A. muciniphila* positively influences anxiety-like behaviour and anhedonia after chronic social defeat stress (McGaughey et al., 2019). Interestingly, the increased relative abundances in R+ animals of *P. distasonis*, a bacterium with potential immunomodulatory properties (Kverka et al., 2011), and *B. acidifaciens*, whose abundance is reportedly decreased after social stress (Bailey et al., 2011), were in agreement with previous findings. Lastly, we observed baseline differences

in the abundance of the phyla Bacteroidetes, Firmicutes and Deferribacteres. Given the influence that the microbiome exerts on brain functions related to the stress response, these observed differences prior to trauma might be indicative of existing predisposition to stress and/or stress reactivity among the trauma-exposed individuals. This finding is especially relevant because shifts in the abundance of these phyla in response to stress have been reported before (Gautam et al., 2018). However, further research is required to establish the relationships between the different taxa within the gut microbial community, how global and regional changes in the composition of the gut microbiome modulate the host's physiology and how different microbial taxa can shape the individual's predisposition to stress prior to any stressful stimulus.

We were also interested in studying the long-term molecular changes that differentiate the R+ and R− phenotypes. Therefore, we performed lipidomic and expression analyses from different brain regions 6 weeks after trauma. We analysed phospholipid levels given their involvement in neural function and signalling (Moreno-Fernandez et al., 2018). The lipidomic data from the dorsal CA hippocampal region revealed that R+ individuals had increased levels of the prohomeostasis lipids sphingomyelin and sphingosine-1-phosphate (Huston et al., 2016) as compared with R− mice. In the dorsal DG, resilient mice showed increased levels of phosphatidylglycerol, and phosphatidylserine, which exerts neuroprotective effects against stress (Hellhammer et al., 2014). Interestingly, our multiomics analysis correlated the lipids phosphatidylglycerol 38:5 and phosphatidylserine 38:4 with a reduced expression of CB_2 receptors in R− mice. This correlation could indicate a role of these receptors in stress-related disorders together with neuroprotective lipids, although more research is required to elaborate on this correlation. Lysophosphatidylinositol, which is known to increase the permeability of the blood–brain barrier via the activation of GPR55 (Leo et al., 2019), was also increased in R+ individuals. Interestingly, significant differences in phosphatidylglycerol, phosphatidylserine and lysophosphatidylinositol between R+ and R− mice were also present in the dorsal CA, but in contrast, R− showed increased levels in this region. Moreover, we did not find differences in AEA or 2-AG levels or their ratio in the dorsal hippocampal regions. However, we observed increased levels of AEA in the PFC of R− animals (Table S4). Although acute stress is known to reduce AEA levels rapidly in hippocampus and amygdala (Bassir Nia et al., 2019), this decrease has not been consistently observed in the PFC (Gray et al., 2015; Hill et al., 2011). Furthermore, most research on the topic of the ECS and PTSD has focused on molecular changes around the time of trauma; thus, the long-term effects in endocannabinoid levels in different brain regions have not been in the focus of research. Our results suggest pro-resilience mechanisms involving phospholipids within the different hippocampal subregions but also that specific lipid molecules contain different physiological functions in different brain regions.

The transcriptomic profiling revealed differences in the dorsal subregions of the hippocampus; the neuropeptide cortistatin, which has anti-inflammatory properties (Delgado & Gonzalez-Rey, 2017), was significantly increased in the dorsal DG of R+ mice as compared with R− animals (Table S5). This observation suggests increased anti-inflammatory properties in R− mice, most likely as a compensation to the trauma. Furthermore, the mRNA levels of some ECS genes were reduced in the dorsal hippocampus of R− mice. The mRNAs for the enzymes responsible for the synthesis and degradation of AEA (NAPE-PLD and FAAH, respectively) were dysregulated in the dorsal CA, together with DAGLα, which synthesizes 2-AG. However, no differences in levels of endocannabinoids observed in this brain region. Additionally, the mRNA encoding the CB_2 receptor was also decreased in the dorsal CA of R− animals, whereas that encoding the CB_1 receptor showed a trend towards the same reduction, albeit not significant. This trend towards reduced mRNA in R− samples was observed for CB_2 receptor in the dorsal DG. It is however noteworthy to mention that both reduced expression of mRNA encoding the CB_1 receptor in the dorsal CA and encoding the CB_2 receptos in the dorsal DG were identified as predictive molecular features of the R− phenotype in the integrative multiomics analysis. Our findings suggest a dysregulation of the ECS in the dorsal hippocampus that might contribute to the maintenance of the pathological state, given the role of the hippocampus in regulating multiple neural functions by integration into many other brain regions. Moreover, the observed differences in expression of the mRNA encoding the CB_2 receptor could be indicative of an unexplored role of these receptors in stress-related disorders. However, whether these differences reflect changes in the CB_2 receptor protein in glial cells or neurons remains to be investigated.

On the other hand, the mRNA levels of several genes relevant to the stress response were increased in the PFC of R− individuals. Among these genes, we found those for receptors such as the Y_5 receptor, a neuropeptide receptor strongly involved in stress-induced maladaptive behaviours (Sah & Geracioti, 2013) and resilience (Sajdyk et al., 2008), for the CRH$_2$ receptor, involved in the HPA axis and anxiety behaviour (Bale & Vale, 2004) and correlated with the severity of PTSD symptoms (Zhang et al., 2020), and the glucocorticoid receptor, the main regulators of the stress response and whose increased levels have been linked with PTSD (Li et al., 2020). We additionally found increased levels in the PFC of the mRNA encoding acid sphingomyelinase, whose activity was shown to be associated with reduced extinction learning (Huston et al., 2016). Furthermore, we measured an increase in mRNA for the CREB-binding protein, an epigenetic regulator of transcription that is involved in various neuronal functions (Barrett et al., 2011; Valor et al., 2011) and whose deletion has shown to promote resilience (Manners et al., 2019) and neurogenesis in the hippocampus (Gundersen et al., 2013). Moreover, we observed increased levels in the PFC of R− mice of mRNA for the enzyme responsible for synthetizing GABA, glutamic acid decarboxylase 2 (GAD2), whose function is essential for proper neuronal communication and correct fear coping (Kutlu et al., 2018). Interestingly, mice lacking GAD2 (GAD2$^{-/-}$) have shown increased susceptibility to stress (Qi et al., 2018), whereas heterozygous mice (GAD2$^{+/-}$) showed increased resilience (Müller et al., 2014). These observations highlight the complex interactions between neuronal excitation and inhibition, and how they can affect the behavioural response to stress. These data suggest that the trauma model we

used induced long-term alterations in the transcription levels of distinct genes, which are indicative of neurobiological systems or pathways that are essential for brain homeostasis and for the correct processing of the traumatic experiences. It would certainly be of interest to investigate whether the dysregulation in gene expression is present before the exposure to trauma or is a consequence thereof, and if so, when exactly the observed dysregulation affects each brain region.

Lastly, our multiomics integrative approach revealed that R+ and R− animals were associated with their own distinct molecular signatures driven by specific changes in the transcriptome, lipidome and gut microbiome. This observation strengthens our behavioural profiling, as we could ascertain that the phenotypes we identified within the trauma-exposed group, based on their behaviour, are also profoundly different at the molecular level. Furthermore, the correlation network analysis of the features important for discriminating resilient and susceptible animals highlighted numerous strong associations between molecular markers even across different omics domains. Interestingly, the correlations between the lipidome and the transcriptome were more abundant and stronger than any correlation between the microbiome and the other biological systems studied here. A possible explanation for this observation could be that the effects of the gut microbiome on brain physiology are only exerted via intermediary molecules, whereas the lipidome and transcriptome exert their function within the same organ. However, it is important to note that the gut microbiome appears to have a stronger association with the brain lipidome than with the transcriptome. These findings demonstrate the complexity and intricacy of the physiological processes that underlie PTSD and stress-related disorders and hint towards potential predictive biomarkers and targets for pharmacological interventions.

ACKNOWLEDGEMENTS

AUTHOR CONTRIBUTIONS

D.P.C. and B.L. designed the project and experiments; D.P.C. performed all the behavioural experiments, tissue collection, RNA extraction and RT-qPCR experiments; R.L. and L.B. helped in the design of the lipidomic analysis and performed the lipid extraction and analysis of the data; L.I. extracted the bacterial DNA for the microbiome analysis; H.T. performed all the bioinformatic analyses with inputs from S.G.; D.P.C. and H.T. wrote the manuscript; and B.L. and S.G. edited the manuscript and supervised the study.

CONFLICT OF INTEREST

The authors declare no conflicts of interest.

DECLARATION OF TRANSPARENCY AND SCIENTIFIC RIGOUR

This Declaration acknowledges that this paper adheres to the principles for transparent reporting and scientific rigour of preclinical research as stated in the *BJP* guidelines for Design & Analysis and Animal Experimentation and as recommended by funding agencies, publishers and other organizations engaged with supporting research.

DATA AVAILABILITY STATEMENT

The data that support the findings of this study are available from the corresponding author upon request.

ORCID

Diego Pascual Cuadrado https://orcid.org/0000-0002-6170-4330

REFERENCES

Alexander, S. P., Christopoulos, A., Davenport, A. P., Kelly, E., Mathie, A., Peters, J. A., Veale, E. L., Armstrong, J. F., Faccenda, E., Harding, S. D., Pawson, A. J., Southan, C., Davies, J. A., Abbracchio, M. P., Alexander, W., Al-hosaini, K., Bäck, M., Barnes, N. M., Bathgate, R., … Ye, R. D. (2021). THE CONCISE GUIDE TO PHARMACOLOGY 2021/22: G protein-coupled receptors. *British Journal of Pharmacology*, *178*(S1), S27–S156. https://doi.org/10.1111/bph.15538

Alexander, S. P., Cidlowski, J. A., Kelly, E., Mathie, A., Peters, J. A., Veale, E. L., Armstrong, J. F., Faccenda, E., Harding, S. D., Pawson, A. J., Southan, C., Davies, J. A., Coons, L., Fuller, P. J., Korach, K. S., & Young, M. J. (2021). THE CONCISE GUIDE TO PHARMACOLOGY 2021/22: Nuclear hormone receptors. *British Journal of Pharmacology*, *178*(S1), S246–S263. https://doi.org/10.1111/bph.15540

Alexander, S. P., Fabbro, D., Kelly, E., Mathie, A., Peters, J. A., Veale, E. L., Armstrong, J. F., Faccenda, E., Harding, S. D., Pawson, A. J., Southan, C., Davies, J. A., Boison, D., Burns, K. E., Dessauer, C., Gertsch, J., Helsby, N. A., Izzo, A. A., Koesling, D., … Wong, S. S. (2021). THE CONCISE GUIDE TO PHARMACOLOGY 2021/22: Enzymes. *British Journal of Pharmacology*, *178*(S1), S313–S411. https://doi.org/10.1111/bph.15542

Alexander, S. P., Kelly, E., Mathie, A., Peters, J. A., Veale, E. L., Armstrong, J. F., Faccenda, E., Harding, S. D., Pawson, A. J., Southan, C., Buneman, O. P., Cidlowski, J. A., Christopoulos, A., Davenport, A. P., Fabbro, D., Spedding, M., Striessnig, J., Davies, J. A., Ahlers-Dannen, K. E., … Zolghadri, Y. (2021). THE CONCISE GUIDE TO PHARMACOLOGY 2021/22: Other Protein Targets. *British Journal of Pharmacology*, *178*(S1), S1–S26. https://doi.org/10.1111/bph.15537

American Psychiatric Association (Ed.). (2013). *Diagnostic and statistical manual of mental disorders: DSM-5* (5th ed.). American Psychiatric Association. 10.1176/appi.books.9780890425596

Asok, A., Kandel, E. R., & Rayman, J. B. (2018). The neurobiology of fear generalization. *Frontiers in Behavioral Neuroscience*, *12*, 329. https://doi.org/10.3389/fnbeh.2018.00329

Bailey, M. T., Dowd, S. E., Galley, J. D., Hufnagle, A. R., Allen, R. G., & Lyte, M. (2011). Exposure to a social stressor alters the structure of the intestinal microbiota: Implications for stressor-induced immunomodulation. *Brain, Behavior, and Immunity*, *25*(3), 397–407. https://doi.org/10.1016/j.bbi.2010.10.023

Bale, T. L., & Vale, W. W. (2004). CRF and CRF receptors: Role in stress responsivity and other behaviors. *Annual Review of Pharmacology and

Toxicology, 44, 525–557. https://doi.org/10.1146/annurev.pharmtox.44.101802.121410

Barrett, R. M., Malvaez, M., Kramar, E., Matheos, D. P., Arrizon, A., Cabrera, S. M., Lynch, G., Greene, R. W., & Wood, M. A. (2011). Hippocampal focal knockout of CBP affects specific histone modifications, long-term potentiation, and long-term memory. Neuropsychopharmacology: Official Publication of the American College of Neuropsychopharmacology, 36(8), 1545–1556. https://doi.org/10.1038/npp.2011.61

Bassir Nia, A., Bender, R., & Harpaz-Rotem, I. (2019). Endocannabinoid system alterations in posttraumatic stress disorder: A review of developmental and accumulative effects of trauma. Chronic Stress (Thousand Oaks, Calif.), 3, 247054701986409. https://doi.org/10.1177/2470547019864096

Bersanelli, M., Mosca, E., Remondini, D., Giampieri, E., Sala, C., Castellani, G., & Milanesi, L. (2016). Methods for the integration of multi-omics data: Mathematical aspects. BMC Bioinformatics, 17(Suppl 2), 15–15. https://doi.org/10.1186/s12859-015-0857-9

Buczynski, M. W., & Parsons, L. H. (2010). Quantification of brain endocannabinoid levels: Methods, interpretations and pitfalls. British Journal of Pharmacology, 160(3), 423–442. https://doi.org/10.1111/j.1476-5381.2010.00787.x

Chu, C., Murdock, M. H., Jing, D., Won, T. H., Chung, H., Kressel, A. M., Tsaava, T., Addorisio, M. E., Putzel, G. G., Zhou, L., Bessman, N. J., Yang, R., Moriyama, S., Parkhurst, C. N., Li, A., Meyer, H. C., Teng, F., Chavan, S. S., Tracey, K. J., ... Artis, D. (2019). The microbiota regulate neuronal function and fear extinction learning. Nature, 574(7779), 543–548. https://doi.org/10.1038/s41586-019-1644-y

Cowden Hindash, A. H., Lujan, C., Howard, M., O'Donovan, A., Richards, A., Neylan, T. C., & Inslicht, S. S. (2019). Gender differences in threat biases: Trauma type matters in posttraumatic stress disorder. Journal of Traumatic Stress, 32(5), 701–711. https://doi.org/10.1002/jts.22439

Curtis, M. J., Alexander, S., Cirino, G., Docherty, J. R., George, C. H., Giembycz, M. A., Hoyer, D., Insel, P. A., Izzo, A. A., Ji, Y., MacEwan, D. A., Sobey, C. G., Stanford, S. C., Teixeira, M. M., Wonnacott, S., & Ahluwalia, A. (2018). Experimental design and analysis and their reporting II: Updated and simplified guidance for authors and peer reviewers. British Journal of Pharmacology, 175, 987–993. https://doi.org/10.1111/bph.14153

Delgado, M., & Gonzalez-Rey, E. (2017). Role of cortistatin in the stressed immune system. Frontiers of Hormone Research, 48, 110–120. https://doi.org/10.1159/000452910

Dutton, R. C., Maurer, A. J., Sonner, J. M., Fanselow, M. S., Laster, M. J., & Eger, E. I. 2nd (2002). Isoflurane causes anterograde but not retrograde amnesia for Pavlovian fear conditioning. Anesthesiology., 96, 1223–1229.

Faria, R., Santana, M. M., Aveleira, C. A., Simões, C., Maciel, E., Melo, T., Santinha, D., Oliveira, M. M., Peixoto, F., Domingues, P., Cavadas, C., & Domingues, M. R. M. (2014). Alterations in phospholipidomic profile in the brain of mouse model of depression induced by chronic unpredictable stress. Neuroscience, 273, 1–11. https://doi.org/10.1016/j.neuroscience.2014.04.042

Fidalgo, A. R., Cibelli, M., White, J. P., Nagy, I., Wan, Y., & Ma, D. (2012). Isoflurane causes neocortical but not hippocampal-dependent memory impairment in mice. Acta Anaesthesiologica Scandinavica, 56, 1052–1057.

Flandreau, E., Risbrough, V., Lu, A., Ableitner, M., Geyer, M. A., Holsboer, F., & Deussing, J. M. (2015). Cell type-specific modifications of corticotropin-releasing factor (CRF) and its type 1 receptor (CRF1) on startle behavior and sensorimotor gating. Psychoneuroendocrinology, 53, 16–28. https://doi.org/10.1016/j.psyneuen.2014.12.005

Gautam, A., Kumar, R., Chakraborty, N., Muhie, S., Hoke, A., Hammamieh, R., & Jett, M. (2018). Altered fecal microbiota composition in all male aggressor-exposed rodent model simulating features of

post-traumatic stress disorder. Journal of Neuroscience Research, 96(7), 1311–1323. https://doi.org/10.1002/jnr.24229

Grassi, S., Mauri, L., Prioni, S., Cabitta, L., Sonnino, S., Prinetti, A., & Giussani, P. (2019). Sphingosine 1-phosphate receptors and metabolic enzymes as druggable targets for brain diseases. Frontiers in Pharmacology, 10, 807. https://doi.org/10.3389/fphar.2019.00807

Gray, J. M., Vecchiarelli, H. A., Morena, M., Lee, T. T. Y., Hermanson, D. J., Kim, A. B., McLaughlin, R. J., Hassan, K. I., Kühne, C., Wotjak, C. T., Deussing, J. M., Patel, S., & Hill, M. N. (2015). Corticotropin-releasing hormone drives anandamide hydrolysis in the amygdala to promote anxiety. The Journal of Neuroscience: The Official Journal of the Society for Neuroscience, 35(9), 3879–3892. https://doi.org/10.1523/JNEUROSCI.2737-14.2015

Guina, J., Baker, M., Stinson, K., Maust, J., Coles, J., & Broderick, P. (2017). Should posttraumatic stress be a disorder or a specifier? Towards improved nosology within the DSM categorical classification system. Current Psychiatry Reports, 19(10), 1–11. https://doi.org/10.1007/s11920-017-0821-7

Gundersen, B. B., Briand, L. A., Onksen, J. L., Lelay, J., Kaestner, K. H., & Blendy, J. A. (2013). Increased hippocampal neurogenesis and accelerated response to antidepressants in mice with specific deletion of CREB in the hippocampus: Role of cAMP response-element modulator τ. The Journal of Neuroscience: The Official Journal of the Society for Neuroscience, 33(34), 13673–13685. https://doi.org/10.1523/JNEUROSCI.1669-13.2013

Hellhammer, J., Vogt, D., Franz, N., Freitas, U., & Rutenberg, D. (2014). A soy-based phosphatidylserine/phosphatidic acid complex (PAS) normalizes the stress reactivity of hypothalamus-pituitary-adrenal-axis in chronically stressed male subjects: A randomized, placebo-controlled study. Lipids in Health and Disease, 13, 121. https://doi.org/10.1186/1476-511X-13-121

Herman, J. P., McKlveen, J. M., Ghosal, S., Kopp, B., Wulsin, A., Makinson, R., Scheimann, J., & Myers, B. (2016). Regulation of the hypothalamic-pituitary-adrenocortical stress response. Comprehensive Physiology, 6(2), 603–621. https://doi.org/10.1002/cphy.c150015

Hewel, C., Kaiser, J., Wierczeiko, A., Linke, J., Reinhardt, C., Endres, K., & Gerber, S. (2019). Common miRNA patterns of Alzheimer's disease and Parkinson's disease and their putative impact on commensal gut microbiota. Frontiers in Neuroscience, 13, 113. https://doi.org/10.3389/fnins.2019.00113

Hill, M. N., McLaughlin, R. J., Pan, B., Fitzgerald, M. L., Roberts, C. J., Lee, T. T.-Y., Karatsoreos, I. N., Mackie, K., Viau, V., Pickel, V. M., McEwen, B. S., Liu, Q., Gorzalka, B. B., & Hillard, C. J. (2011). Recruitment of prefrontal cortical endocannabinoid signaling by glucocorticoids contributes to termination of the stress response. The Journal of Neuroscience: The Official Journal of the Society for Neuroscience, 31(29), 10506–10515. https://doi.org/10.1523/JNEUROSCI.0496-11.2011

Hill, M. N., Miller, G. E., Carrier, E. J., Gorzalka, B. B., & Hillard, C. J. (2009). Circulating endocannabinoids and N-acyl ethanolamines are differentially regulated in major depression and following exposure to social stress. Psychoneuroendocrinology, 34(8), 1257–1262. https://doi.org/10.1016/j.psyneuen.2009.03.013

Hillard, C. J. (2018). Circulating endocannabinoids: From whence do they come and where are they going? Neuropsychopharmacology: Official Publication of the American College of Neuropsychopharmacology, 43(1), 155–172. https://doi.org/10.1038/npp.2017.130

Hoban, A. E., Stilling, R. M., Moloney, G., Shanahan, F., Dinan, T. G., Clarke, G., & Cryan, J. F. (2018). The microbiome regulates amygdala-dependent fear recall. Molecular Psychiatry, 23(5), 1134–1144. https://doi.org/10.1038/mp.2017.100

Horn, S. R., & Feder, A. (2018). Understanding resilience and preventing and treating PTSD. Harvard Review of Psychiatry, 26(3), 158–174. https://doi.org/10.1097/HRP.0000000000000194

Huo, R., Zeng, B., Zeng, L., Cheng, K., Li, B., Luo, Y., Wang, H., Zhou, C., Fang, L., Li, W., Niu, R., Wei, H., & Xie, P. (2017). Microbiota modulate

anxiety-like behavior and endocrine abnormalities in hypothalamic-pituitary-adrenal axis. *Frontiers in Cellular and Infection Microbiology*, 7, 489. https://doi.org/10.3389/fcimb.2017.00489

Huston, J. P., Kornhuber, J., Mühle, C., Japtok, L., Komorowski, M., Mattern, C., Reichel, M., Gulbins, E., Kleuser, B., Topic, B., De Souza Silva, M. A., & Müller, C. P. (2016). A sphingolipid mechanism for behavioral extinction. *Journal of Neurochemistry*, 137(4), 589–603. https://doi.org/10.1111/jnc.13537

Jarzimski, C., Karst, M., Zoerner, A. A., Rakers, C., May, M., Suchy, M. T., Tsikas, D., Krauss, J. K., Scheinichen, D., Jordan, J., & Engeli, S. (2012). Changes of blood endocannabinoids during anaesthesia: a special case for fatty acid amide hydrolase inhibition by propofol? *British Journal of Clinical Pharmacology*, 74, 54–59.

Jeong, M.-J., Lee, C., Sung, K., Jung, J. H., Pyo, J. H., & Kim, J.-H. (2020). Fear response-based prediction for stress susceptibility to PTSD-like phenotypes. *Molecular Brain*, 13(1), 1–9. https://doi.org/10.1186/s13041-020-00667-5

Kelly, J. R., Kennedy, P. J., Cryan, J. F., Dinan, T. G., Clarke, G., & Hyland, N. P. (2015). Breaking down the barriers: The gut microbiome, intestinal permeability and stress-related psychiatric disorders. *Frontiers in Cellular Neuroscience*, 9, 392. https://doi.org/10.3389/fncel.2015.00392

Kokras, N., & Dalla, C. (2014). Sex differences in animal models of psychiatric disorders. *British Journal of Pharmacology*, 171(20), 4595–4619. https://doi.org/10.1111/bph.12710

Kutlu, M. G., Connor, D. A., Tumolo, J. M., Cann, C., Garrett, B., & Gould, T. J. (2018). Nicotine modulates contextual fear extinction through changes in ventral hippocampal GABAergic function. *Neuropharmacology*, 141, 192–200. https://doi.org/10.1016/j.neuropharm.2018.08.019

Kverka, M., Zakostelska, Z., Klimesova, K., Sokol, D., Hudcovic, T., Hrncir, T., Rossmann, P., Mrazek, J., Kopecny, J., Verdu, E. F., & Tlaskalova-Hogenova, H. (2011). Oral administration of *Parabacteroides distasonis* antigens attenuates experimental murine colitis through modulation of immunity and microbiota composition. *Clinical and Experimental Immunology*, 163(2), 250–259. https://doi.org/10.1111/j.1365-2249.2010.04286.x

Leo, L. M., Familusi, B., Hoang, M., Smith, R., Lindenau, K., Sporici, K. T., Brailoiu, E., Abood, M. E., & Brailoiu, G. C. (2019). GPR55-mediated effects on brain microvascular endothelial cells and the blood–brain barrier. *Neuroscience*, 414, 88–98. https://doi.org/10.1016/j.neuroscience.2019.06.039

Lerner, R., Pascual Cuadrado, D., Post, J. M., Lutz, B., & Bindila, L. (2019). Broad lipidomic and transcriptional changes of prophylactic PEA administration in adult mice. *Frontiers in Neuroscience*, 13, 527. https://doi.org/10.3389/fnins.2019.00527

Lerner, R., Post, J. M., Ellis, S. R., Vos, D. R. N., Heeren, R. M. A., Lutz, B., & Bindila, L. (2018). Simultaneous lipidomic and transcriptomic profiling in mouse brain punches of acute epileptic seizure model compared to controls. *Journal of Lipid Research*, 59(2), 283–297. https://doi.org/10.1194/jlr.M080093

Li, H., Su, P., Lai, T. K., Jiang, A., Liu, J., Zhai, D., Campbell, C. T., Lee, F. H., Yong, W., Pasricha, S., Li, S., Wong, A. H., Ressler, K. J., & Liu, F. (2020). The glucocorticoid receptor–FKBP51 complex contributes to fear conditioning and posttraumatic stress disorder. *The Journal of Clinical Investigation*, 130(2), 877–889. https://doi.org/10.1172/JCI130363

Lilley, E., Stanford, S. C., Kendall, D. E., Alexander, S. P. H., Cirino, G., Docherty, J. R., George, C. H., Insel, P. A., Izzo, A. A., Ji, Y., Panettieri, R. A., Sobey, C. G., Stefanska, B., Stephens, G., Teixeira, M., & Ahluwalia, A. (2020). ARRIVE 2.0 and the British Journal of Pharmacology: Updated guidance for 2020. *British Journal of Pharmacology*, 177, 3611–3616. https://doi.org/10.1111/bph.15178

Lin, D., & Zuo, Z. (2011). Isoflurane induces hippocampal cell injury and cognitive impairments in adult rats. *Neuropharmacology*, 61, 1354–1349.

Liu, M.-Y., Yin, C.-Y., Zhu, L.-J., Zhu, X.-H., Xu, C., Luo, C.-X., Chen, H., Zhu, D.-Y., & Zhou, Q.-G. (2018). Sucrose preference test for measurement of stress-induced anhedonia in mice. *Nature Protocols*, 13(7), 1686–1698. https://doi.org/10.1038/s41596-018-0011-z

Liu, S., da Cunha, A. P., Rezende, R. M., Cialic, R., Wei, Z., Bry, L., Comstock, L. E., Gandhi, R., & Weiner, H. L. (2016). The host shapes the gut microbiota via fecal microRNA. *Cell Host & Microbe*, 19(1), 32–43. https://doi.org/10.1016/j.chom.2015.12.005

Manners, M. T., Brynildsen, J. K., Schechter, M., Liu, X., Eacret, D., & Blendy, J. A. (2019). CREB deletion increases resilience to stress and downregulates inflammatory gene expression in the hippocampus. *Brain, Behavior, and Immunity*, 81, 388–398. https://doi.org/10.1016/j.bbi.2019.06.035

McGaughey, K. D., Yilmaz-Swenson, T., Elsayed, N. M., Cruz, D. A., Rodriguiz, R. M., Kritzer, M. D., Peterchev, A. V., Roach, J., Wetsel, W. C., & Williamson, D. E. (2019). Relative abundance of *Akkermansia* spp. and other bacterial phylotypes correlates with anxiety- and depressive-like behavior following social defeat in mice. *Scientific Reports*, 9(1), 3281. https://doi.org/10.1038/s41598-019-40140-5

Menard, C., Pfau, M. L., Hodes, G. E., Kana, V., Wang, V. X., Bouchard, S., Takahashi, A., Flanigan, M. E., Aleyasin, H., LeClair, K. B., Janssen, W. G., Labonté, B., Parise, E. M., Lorsch, Z. S., Golden, S. A., Heshmati, M., Tamminga, C., Turecki, G., Campbell, M., ... Russo, S. J. (2017). Social stress induces neurovascular pathology promoting depression. *Nature Neuroscience*, 20(12), 1752–1760. https://doi.org/10.1038/s41593-017-0010-3

Mo, A., Mukamel, E. A., Davis, F. P., Luo, C., Henry, G. L., Picard, S., Urich, M. A., Nery, J. R., Sejnowski, T. J., Lister, R., Eddy, S. R., Ecker, J. R., & Nathans, J. (2015). Epigenomic signatures of neuronal diversity in the mammalian brain. *Neuron*, 86(6), 1369–1384. https://doi.org/10.1016/j.neuron.2015.05.018

Morena, M., Berardi, A., Colucci, P., Palmery, M., Trezza, V., Hill, M. N., & Campolongo, P. (2018). Enhancing endocannabinoid neurotransmission augments the efficacy of extinction training and ameliorates traumatic stress-induced behavioral alterations in rats. *Neuropsychopharmacology: Official Publication of the American College of Neuropsychopharmacology*, 43(6), 1284–1296. https://doi.org/10.1038/npp.2017.305

Moreno-Fernandez, R. D., Tabbai, S., Castilla-Ortega, E., Perez-Martin, M., Estivill-Torrus, G., Rodriguez de Fonseca, F., Santin, L. J., & Pedraza, C. (2018). Stress, depression, resilience and ageing: A role for the LPA-LPA1 pathway. *Current Neuropharmacology*, 16(3), 271–283. https://doi.org/10.2174/1570159X15666170710200352

Muir, J., Lorsch, Z. S., Ramakrishnan, C., Deisseroth, K., Nestler, E. J., Calipari, E. S., & Bagot, R. C. (2018). In vivo fiber photometry reveals signature of future stress susceptibility in nucleus accumbens. *Neuropsychopharmacology: Official Publication of the American College of Neuropsychopharmacology*, 43(2), 255–263. https://doi.org/10.1038/npp.2017.122

Müller, I., Obata, K., Richter-Levin, G., & Stork, O. (2014). GAD65 haplodeficiency conveys resilience in animal models of stress-induced psychopathology. *Frontiers in Behavioral Neuroscience*, 8, 265. https://doi.org/10.3389/fnbeh.2014.00265

Nievergelt, C. M., Maihofer, A. X., Klengel, T., Atkinson, E. G., Chen, C.-Y., Choi, K. W., Coleman, J. R. I., Dalvie, S., Duncan, L. E., Gelernter, J., Levey, D. F., Logue, M. W., Polimanti, R., Provost, A. C., Ratanatharathorn, A., Stein, M. B., Torres, K., Aiello, A. E., Almli, L. M., ... Koenen, K. C. (2019). International meta-analysis of PTSD genome-wide association studies identifies sex- and ancestry-specific genetic risk loci. *Nature Communications*, 10(1), 4558. https://doi.org/10.1038/s41467-019-12576-w

Percie du Sert, N., Hurst, V., Ahluwalia, A., Alam, S., Avey, M. T., Baker, M., Browne, W. J., Clark, A., Cuthill, I. C., Dirnagl, U., Emerson, M., Garner, P., Holgate, S. T., Howells, D. W., Karp, N. A., Lazic, S. E.,

Lidster, K., MacCallum, C. J., Macleod, M., ... Würbel, H. (2020). The ARRIVE guidelines 2.0: Updated guidelines for reporting animal research. *PLoS Biology*, 18(7), e3000410. https://doi.org/10.1371/journal.pbio.3000410

Qi, J., Kim, M., Sanchez, R., Ziaee, S. M., Kohtz, J. D., & Koh, S. (2018). Enhanced susceptibility to stress and seizures in GAD65 deficient mice. *PLoS ONE*, 13(1), e0191794. https://doi.org/10.1371/journal.pone.0191794

Rakesh, G., Morey, R. A., Zannas, A. S., Malik, Z., Marx, C. E., Clausen, A. N., Kritzer, M. D., & Szabo, S. T. (2019). Resilience as a translational endpoint in the treatment of PTSD. *Molecular Psychiatry*, 24(9), 1268–1283. https://doi.org/10.1038/s41380-019-0383-7

Reber, S. O., Siebler, P. H., Donner, N. C., Morton, J. T., Smith, D. G., Kopelman, J. M., Lowe, K. R., Wheeler, K. J., Fox, J. H., Hassell, J. E., Greenwood, B. N., Jansch, C., Lechner, A., Schmidt, D., Uschold-Schmidt, N., Füchsl, A. M., Langgartner, D., Walker, F. R., Hale, M. W., ... Lowry, C. A. (2016). Immunization with a heat-killed preparation of the environmental bacterium *Mycobacterium vaccae* promotes stress resilience in mice. *Proceedings of the National Academy of Sciences of the United States of America*, 113(22), E3130–E3139. https://doi.org/10.1073/pnas.1600324113

Rey, A. A., Purrio, M., Viveros, M.-P., & Lutz, B. (2012). Biphasic effects of cannabinoids in anxiety responses: CB_1 and $GABA_B$ receptors in the balance of GABAergic and glutamatergic neurotransmission. *Neuropsychopharmacology: Official Publication of the American College of Neuropsychopharmacology*, 37(12), 2624–2634. https://doi.org/10.1038/npp.2012.123

Richter-Levin, G., Stork, O., & Schmidt, M. V. (2019). Animal models of PTSD: A challenge to be met. *Molecular Psychiatry*, 24(8), 1135–1156. https://doi.org/10.1038/s41380-018-0272-5

Ruffini, N., Klingenberg, S., Schweiger, S., & Gerber, S. (2020). Common factors in neurodegeneration: A meta-study revealing shared patterns on a multi-omics scale. *Cell*, 9(12), 2642. https://doi.org/10.3390/cells9122642

Sah, R., & Geracioti, T. D. (2013). Neuropeptide Y and posttraumatic stress disorder. *Molecular Psychiatry*, 18(6), 646–655. https://doi.org/10.1038/mp.2012.101

Sajdyk, T. J., Johnson, P. L., Leitermann, R. J., Fitz, S. D., Dietrich, A., Morin, M., Gehlert, D. R., Urban, J. H., & Shekhar, A. (2008). Neuropeptide Y in the amygdala induces long-term resilience to stress-induced reductions in social responses but not hypothalamic–adrenal–pituitary axis activity or hyperthermia. *The Journal of Neuroscience: The Official Journal of the Society for Neuroscience*, 28(4), 893–903. https://doi.org/10.1523/JNEUROSCI.0659-07.2008

Sauerhöfer, E., Pamplona, F. A., Bedenk, B., Moll, G. H., Dawirs, R. R., von Hörsten, S., Wotjak, C. T., & Golub, Y. (2012). Generalization of contextual fear depends on associative rather than non-associative memory components. *Behavioural Brain Research*, 233(2), 483–493. https://doi.org/10.1016/j.bbr.2012.05.016

Sbarski, B., & Akirav, I. (2020). Cannabinoids as therapeutics for PTSD. *Pharmacology & Therapeutics*, 211, 107551. https://doi.org/10.1016/j.pharmthera.2020.107551

Schelling, G., Hauer, D., Azad, S. C., Schmoelz, M., Chouker, A., Schmidt, M., Hornuss, C., Rippberger, M., Briegel, J., Thiel, M., & Vogeser, M. (2006). Effects of general anesthesia on anandamide blood levels in humans. *Anesthesiology*, 104, 273–277.

Shoji, H., Takao, K., Hattori, S., & Miyakawa, T. (2014). Contextual and cued fear conditioning test using a video analyzing system in mice. *Journal of Visualized Experiments: JoVE*, (85), e50871. https://doi.org/10.3791/50871

Siegmund, A., & Wotjak, C. T. (2007). A mouse model of posttraumatic stress disorder that distinguishes between conditioned and sensitised fear. *Journal of Psychiatric Research*, 41(10), 848–860. https://doi.org/10.1016/j.jpsychires.2006.07.017

Sudo, N., Chida, Y., Aiba, Y., Sonoda, J., Oyama, N., Yu, X.-N., Kubo, C., & Koga, Y. (2004). Postnatal microbial colonization programs the hypothalamic–pituitary–adrenal system for stress response in mice. *The Journal of Physiology*, 558(Pt 1), 263–275. https://doi.org/10.1113/jphysiol.2004.063388

Thoeringer, C. K., Henes, K., Eder, M., Dahlhoff, M., Wurst, W., Holsboer, F., Deussing, J. M., Moosmang, S., & Wotjak, C. T. (2012). Consolidation of remote fear memories involves Corticotropin-Releasing Hormone (CRH) receptor type 1-mediated enhancement of AMPA receptor GluR1 signaling in the dentate gyrus. *Neuropsychopharmacology: Official Publication of the American College of Neuropsychopharmacology*, 37(3), 787–796. https://doi.org/10.1038/npp.2011.256

Torrisi, S. A., Lavanco, G., Maurel, O. M., Gulisano, W., Laudani, S., Geraci, F., Grasso, M., Barbagallo, C., Caraci, F., Bucolo, C., Ragusa, M., Papaleo, F., Campolongo, P., Puzzo, D., Drago, F., Salomone, S., & Leggio, G. M. (2021). A novel arousal-based individual screening reveals susceptibility and resilience to PTSD-like phenotypes in mice. *Neurobiology of Stress*, 14, 100286. https://doi.org/10.1016/j.ynstr.2020.100286

Valor, L. M., Pulopulos, M. M., Jimenez-Minchan, M., Olivares, R., Lutz, B., & Barco, A. (2011). Ablation of CBP in forebrain principal neurons causes modest memory and transcriptional defects and a dramatic reduction of histone acetylation but does not affect cell viability. *The Journal of Neuroscience: The Official Journal of the Society for Neuroscience*, 31(5), 1652–1663. https://doi.org/10.1523/JNEUROSCI.4737-10.2011

Walter, K. H., Levine, J. A., Highfill-McRoy, R. M., Navarro, M., & Thomsen, C. J. (2018). Prevalence of posttraumatic stress disorder and psychological comorbidities among U.S. active duty service members, 2006–2013. *Journal of Traumatic Stress*, 31(6), 837–844. https://doi.org/10.1002/jts.22337

Weis, F., Beiras-Fernandez, A., Hauer, D., Hornuss, C., Sodian, R., Kreth, S., Briegel, J., & Schelling, G. (2010). Effect of anaesthesia and cardiopulmonary bypass on blood endocannabinoid concentrations during cardiac surgery. *British Journal of Anaesthesia*, 105, 139–144.

Williams, L. M., Kemp, A. H., Felmingham, K., Barton, M., Olivieri, G., Peduto, A., Gordon, E., & Bryant, R. A. (2006). Trauma modulates amygdala and medial prefrontal responses to consciously attended fear. *NeuroImage*, 29(2), 347–357. https://doi.org/10.1016/j.neuroimage.2005.03.047

Zhang, K., Wang, L., Li, G., Cao, C., Fang, R., Liu, P., Luo, S., & Zhang, X. (2020). Correlation between hypothalamic-pituitary-adrenal axis gene polymorphisms and posttraumatic stress disorder symptoms. *Hormones and Behavior*, 117, 104604. https://doi.org/10.1016/j.yhbeh.2019.104604

Zhang, S., Hu, X., Guan, W., Luan, L., Li, B., Tang, Q., & Fan, H. (2017). Isoflurane anesthesia promotes cognitive impairment by inducing expression of β-amyloid protein-related factors in the hippocampus of aged rats. *PLoS ONE*, 12, e0175654.

SUPPORTING INFORMATION

Additional supporting information may be found in the online version of the article at the publisher's website.